Deliverable 2.3b

Stress-induced seismic anisotropy: a promising tool to assess reservoir proprieties and caprock integrity.

Organisation(s)	University of Oxford, British Geological Survey
Author(s)	Joseph Asplet, Tom Kettlety, Mark Fellgett, Mike Kendall.
Reviewer	Brian Baptie (British Geological Survey) Daniel Roberts (Rockfield)
Type of deliverable	Report
Dissemination level	Public
WP	2.4
Issue date	7/11/2024
Document version	1

Keywords:

Stress orientations, Seismic Anisotropy, Shear-wave splitting

Summary:

This deliverable assesses the potential of seismic anisotropy to measure stress within the CO_2 storage complex, primarily the reservoir and overburden. Using onshore passive seismic and stress data for the UK, we test the potential for shear-wave splitting to be used to monitor the stress field in and above CO_2 storage sites. We focus on four regions: Northeast England, Northwest England, Southeast England and South Wales. Stress-induced anisotropy is observed in all regions and is particularly clear in Northwest England and Southeast England.

We also show, for the first time, that shear-wave splitting can be measured using seismicity recorded by offshore Permanent Reservoir Monitoring Systems (PRMs). Shear-wave splitting is measured at select PRM stations at the Snorre field using data recorded from the 21st March 2022 M_W 5.1 Tampen Spur earthquakes and subsequent microseismic aftershocks ($0.1 < \$M_L < 2.6$). These results show that offshore sensors, such as PRM systems, are suitable for measuring shear-wave splitting for microseismic data even in relatively sparse deployments if the sensors are deployed above CO_2 storage projects. This makes shear-wave splitting an important potential added value that should be considered when planning offshore passive seismic monitoring of CO_2 storage projects.

SHARP storage project deliverable 2.3b

Stress-induced seismic anisotropy: a promising tool to assess reservoir proprieties and caprock integrity.

November 2024

Joseph Asplet, Tom Kettlety, Mark Fellgett and Mike Kendall

Contents

Executive summary

Developing additional means of constraining or monitoring stress in the CO_2 storage complex are valuable, particularly methods that are independent means of imaging the reservoir, seal, and overburden units. It is well known that seismic anisotropy can develop in the upper crust due to the preferential alignment of fractures with the maximum horizontal stress direction. Using onshore passive seismic and stress data for the UK, we test the potential for shear-wave splitting to be used to monitor the stress field in and above CO_2 storage sites. We measure shear-wave splitting data for local seismicity with magnitudes ranging from $-1 < M_L < 5$, which encompasses induced microseismicity we may expect to see during CO_2 injection and regional macro-scale earthquakes. Across the UK the measured % anisotropy ranges from $0.354\% < \xi < 19.7\%$. We focus on four regions: Northeast England, Northwest England, South East England and South Wales. At all four regions we observe some signature of stress-induced anisotropy, which is particularly clear in Northwest England at Preston New Road, Lancashire. In South East England, we observe a change in anisotropy across the Newdigate fault and a temporal variation in anisotropy during the Newdigate earthquake sequence. This highlights the potential for shear-wave splitting to measure temporal variations in the stress field.

We also show, for the first time, that shear-wave splitting can be measured using seismicity recorded by offshore Permanent Reservoir Monitoring Systems (PRMs). Shear-wave splitting is measured at select PRM stations at the Snorre field using data recorded from the 21st March 2022 M_W 5.1 Tampen Spur earthquakes and subsequent microseismic aftershocks ($0.1 < M_L < 2.6$). These results show that offshore sensors, such as PRM systems, are suitable for measuring shear-wave splitting for microseismic data even in relatively sparse deployments if the sensors are deployed above CO_2 storage projects. This makes shear-wave splitting an important potential added value that should be considered when planning offshore passive seismic monitoring of CO_2 storage projects.

As shear-wave splitting is a passive measurement, it gives the potential to make semi-continuous measurements of the stress field in the caprock and overburden units, provided there is sufficient microseismicity in underlying formations or basement. However, the potential site specific heterogeneities in anisotropy mean that microseismic monitoring networks must offer good azimuthal coverage of the site. With sufficient instrumentation, and microseismicity to measure, shear-wave splitting offers a tool to extend stress measurements away from boreholes and constitutes an important value-add to offshore microseismic monitoring networks.

1 Introduction

This report presents the work conducted in work package 2.4 of the SHARP Storage project. Work package 2.4 explores if seismic anisotropy, as measured by shear-wave splitting, can be used to assess stress and monitor stress changes in CO_2 storage complexes. In this report we provide an overview of seismic anisotropy, the mechanism by which it develops in response to crustal stress anisotropy, and how anisotropy can be measured using shear-wave splitting.

We use UK onshore passive seismic data to measure shear-wave splitting and compare it to data from the Stress Map of Great Britain and Ireland (Kingdon et al., 2022) to test if shear-wave splitting, measured using local earthquakes, can be used to constrain the orientation of maximum horizontal stress. We then measure shear-wave splitting for data recorded by various offshore systems, including an OBS deployment and Permanent Reservoir Monitoring (PRM) systems deployed at fields in the Northern North Sea to test if shear-wave splitting measurements can be reliably made in offshore projects.

1.1 Stress, caprock integrity, and containment risk

The SHARP Storage project aims to better quantify stress and its uncertainty in the North Sea. The project focuses on regions with proposed sites for CO_2 storage. This is because *in situ* stress state can naturally have a significant impact on the operation and containment risk assessment of storage projects. The likelihood of fault failure, fracture development, and other deformation are affected by stress, and thus it is a critical variable to constrain when assessing a field for CO_2 injection.

Drilling and operating injection wells in regions or depths that may not have had previous hydrocarbon exploration may mean there are fewer data to conduct leakage risk assessments. Additional means of constraining stress or fracturing are valuable, particularly independent geophysical methods to image the reservoir, seal, and overburden units. Fracture and fault trends in particular are important inputs in containment risk assessment, as their orientations with respect to *in situ* stresses significantly affect their potential behaviour when stress changes occur as a result of injection.

1.2 Seismic Anisotropy

Seismic anisotropy refers to a variation in seismic velocity with propagation direction. Anisotropy in the Earth's crust can occur due to various mechanisms operating at different length scales. This can range from the preferential alignments of mineral grains (or crystal preferred orientation, CPO) within a rock formation, to the alignment of heterogeneities, such as sedimentary layering (Backus, 1962) or fracture sets (e.g., Hudson, 1981; Chapman, 2003; Jin et al., 2018), which are smaller than the sampling seismic wavelength.

Despite the wide variety of potential mechanisms, one unifying theme is that they are all expressions of order in materials. Crystal preferred orientation typically develops in high temperature conditions, where crystalline rocks undergo plastic deformation. The resulting anisotropic crystal fabric preserves the strain orientation. In crustal rocks, near-vertical microscale fractures sets aligned with the regional maximum horizontal stress (S_{Hmax}) is accepted as the predominant mechanism for observed seismic anisotropy (e.g., Crampin, 1978; Crampin and Peacock, 2005; Boness and Zoback, 2006). At the Clair

field, anisotropy was shown to be indicative of reservoir quality where observed increasing amplitude variation with offset and azimuth (AVOA) signal could only be explained by increased fracturing with depth (Kendall et al., 2007). In some regions a more complex pattern of anisotropy can be seen where the effect of structural features (e.g., Boness and Zoback, 2006; Hurd and Bohnhoff, 2012; Baird et al., 2015), or the development of multiple fracture sets (Baird et al., 2013) creates an anisotropic fabric that is not completely stress-dependent.

Stress induced seismic anisotropy (or Extensive Dilatancy Anisotropy; e.g., Crampin, 1999) develops in the presence of differential horizontal stresses where microscale cracks preferentially grow or close such that the total fracture set aligns with the maximum horizontal stress. The strength of this preferential alignment is proportional to the ratio of the minimum and maximum horizontal stress, with the aspect ratio and density of aligned cracks increasing with the stress ratio (Crampin, 1999). As aspect ratio and fracture density are the two parameters that primarily control the strength of anisotropy for an aligned fracture set (Hudson, 1981; Chapman, 2003), seismic anisotropy can be sensitive to temporal variations in horizontal stress. Rock physics models incorporating poroelastic squirt flow show that along with microcrack, meso-scale fractures (i.e., fracture significantly larger than the grainsize) control seismic anisotropy where these larger fractures can make the anisotropy frequency-dependent. Where frequency-dependent anisotropy is observed, it is then possible to invert for fracture size and density, which is a useful tool when characterising a reservoir and assessing seal integrity (Al-Harrasi et al., 2011). In this report we do not consider frequency-dependent anisotropy and refer to microcracks and meso-scale fractures collectively as 'cracks'.

1.3 Shear-wave splitting

Shear-wave splitting, or seismic birefringence, occurs when an incident shear-wave propagates through an anisotropic medium. Upon entering the medium the shear-wave is split in two, where one of the shear-waves is polarised along the fast velocity direction, or the fast polarisation direction ϕ_f, and the other along an (assumed) orthogonal direction. These two shear-waves, referred to as the fast (or S1) and slow (or S2) shear-waves, propagate through the medium at different velocities. This introduces a time delay between the two shear-waves, δt, which is preserved along the remainder of the ray path. This time delay depends on both the thickness of the anisotropic medium and the strength of the anisotropy.

Rock physics models with aligned, saturated or unsaturated, microcracks and meso-scale fractures show that ϕ_f is aligned with fracture strike (e.g., Hudson, 1981; Chapman, 2003). Therefore if the fractures develop parallel to S_{Hmax} then ϕ_f can be used as proxy measure for the orientation of S_{Hmax}. Measurements of shear-wave splitting have been used as a proxy for crustal stress, particularly in volcanic settings e.g., Savage et al., 2010b; Baird et al., 2015; Illsley-Kemp et al., 2019. Shear-wave splitting has also been used to measure stress changes due to hydraulic fracturing (e.g., Baird et al., 2013; Igonin et al., 2022), CO_2 injection (e.g., Stork et al., 2015), and surrounding oil fields (e.g., Teanby et al., 2004a). In certain cases, fluid filled fractures may also induce an attenuation anisotropy which can affect shear-wave splitting measurement (Asplet et al., 2024), but also offers the potential to further constrain fracture properties.

One advantage of shear-wave splitting is that, with sufficient instrumentation, measurements can be made at significantly higher spatial and temporal resolutions than borehole breakout analysis, drilling induced tensile fractures or other methods for interpreting horizontal stress orientations. This gives shear-wave splitting the potential to fill gaps between borehole measurement providing a higher-resolution image of the subsurface stress field. As a passive measurement, however, shear-wave splitting does require detectable microseismicity to occur beneath or within reservoir. A source within the reservoir will generate shear-waves that sample the caprock, whilst sources beneath the reservoir will generate shear-waves with sample both reservoir and caprock. At some sites, multiple layers of anisotropy may be observed, which would distort the signal of stress-induced anisotropy. Therefore it is important to have regional stress data to tie shear-wave splitting observations to.

Furthermore, seismic anisotropy can be used to elucidate fracture properties by inverting shear-wave splitting measurements (e.g., Verdon and Kendall, 2011; Al-Harrasi et al., 2011). Inversion of shear-wave splitting dataset directly for anisotropic fabrics is still a nascent field. Recent developments have primarily focused on studying mantle anisotropy (e.g., Wookey, 2012; Asplet et al., 2023; Link and Long, 2024), however frameworks have also been developed for reservoir-scale inversions to identify vertically aligned fractures and horizontal sedimentary fabrics (Verdon et al., 2009). Future work may allow for these methods to be translated for application to measurements of local shear-wave splitting and extended to invert measurements directly for stress anisotropy (i.e., S_{Hmin} / S_{Hmax}).

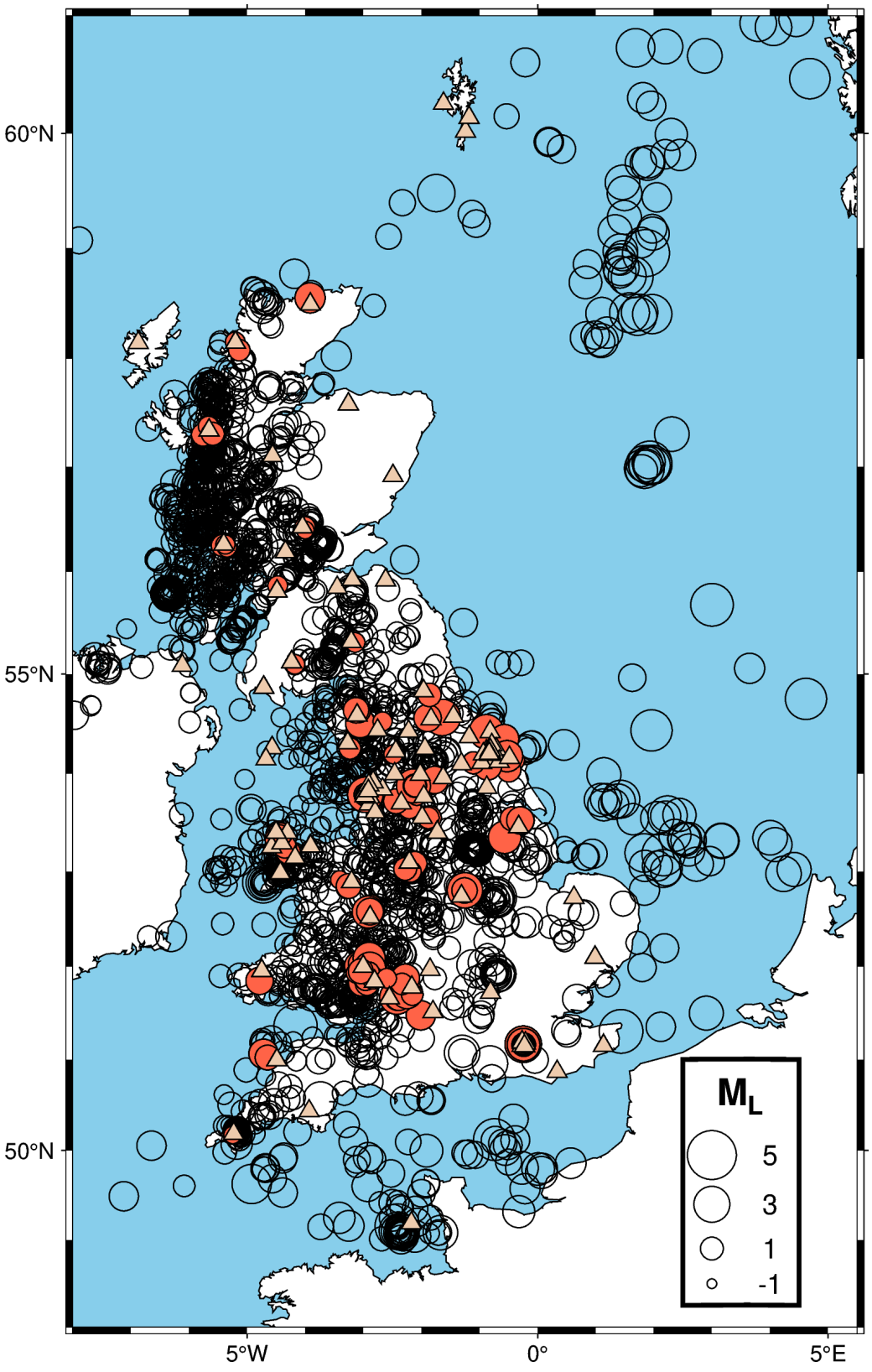

FIGURE 1: Map showing UK earthquakes recorded by the British Geological Survey from 2010 - 2022. Earthquakes which are within the shear-wave window of a station where a S phase are considered viable shear-wave splitting candidates and are shown by the red circles. Earthquakes which are not considered viable candidates are shown by the open circles. Circles are scaled proportional to the local magnitude of each earthquake. Triangles show the location of stations used.

2 Data Used

Shear-wave splitting is measured for several different data sets described below. The majority of data are recorded in the UK, which allows us to compare shear-wave splitting results to the recently complied Stress Map of Great Britain and Ireland 2022 (Kingdon et al., 2022). Data from offshore sensors are then used to test the potential of different offshore monitoring systems to measure shear-wave splitting for detected microseismicity.

Shear-waves are modified by interaction with the free surface (Nuttli, 1961). Booth and Crampin (1985) showed that there is a shear-wave window where incident shear-waves are free from distortion only when the angle of incidence at the free surface is less than the critical angle

$$i_c = \sin^{-1} \frac{V_S}{V_P}, \tag{1}$$

where V_P and V_S are the P-wave and S-wave velocities at the surface (Booth and Crampin, 1985). We assume a critical angle, or shear-wave window, of 45° which is a common assumption in near-surface shear-wave splitting (e.g., Liu et al., 2014). Therefore, we only use data where the earthquake epicentral distance from a receiver is less than or equal to its depth.

2.1 UK onshore seismicity

The UK dataset uses data recorded by broadband seismic stations that form the permanent UK seismic network (GBarray; British Geological Survey, 1970) and a temporary network (UKArray; British Geological Survey, 2015). We search the British Geological Survey (BGS) earthquake catalogue for earthquakes between 2010-2022 recorded at stations with S picks that fall within the 45° shear-wave window assuming a linear ray path for shear-wave arrivals. This dataset is supplemented with microseismic data recorded at broadband surface stations at Preston New Road (Clarke et al., 2019b; Kettlety et al., 2020). Combined, this yields an initial dataset of 3392 earthquakes in the BGS catalogue that lie within the shear-wave window of a station. For many earthquakes in this dataset the waveform data are either unavailable due to a data embargo or no S phase was picked. When these events are disregarded the dataset is reduced to 1452 viable candidate earthquakes for shear-wave splitting analysis. Further data attrition occurs when we add the requirement for earthquakes to be recorded at 3-component broadband seismometers. This results in a dataset of 902 earthquakes which are within the shear-wave window of a 3-component broadband seismic station (Figure 1).

The largest limitation in the usability of publicly available data is the previously described shear-wave window restriction. The vast majority of earthquakes recorded in the UK have a focal depth under 10 km (Figure 2). Whilst the UK is well instrumented the seismic network is sparse, and the majority of the seismicity recorded does not lie within the shear-wave window of a station. Many of the events which do lie within the shear-wave window are recorded by targeted deployment to monitor induced seismicity at Preston New Road, Lancashire, (Clarke et al., 2019b; Kettlety et al., 2020) or a natural earthquake sequence near Newdigate, Surrey (Hicks et al., 2019). This gives the dataset significant geographical heterogeneity, which limits our ability to constrain stress across the the UK but does yield two sites for more detailed case studies.

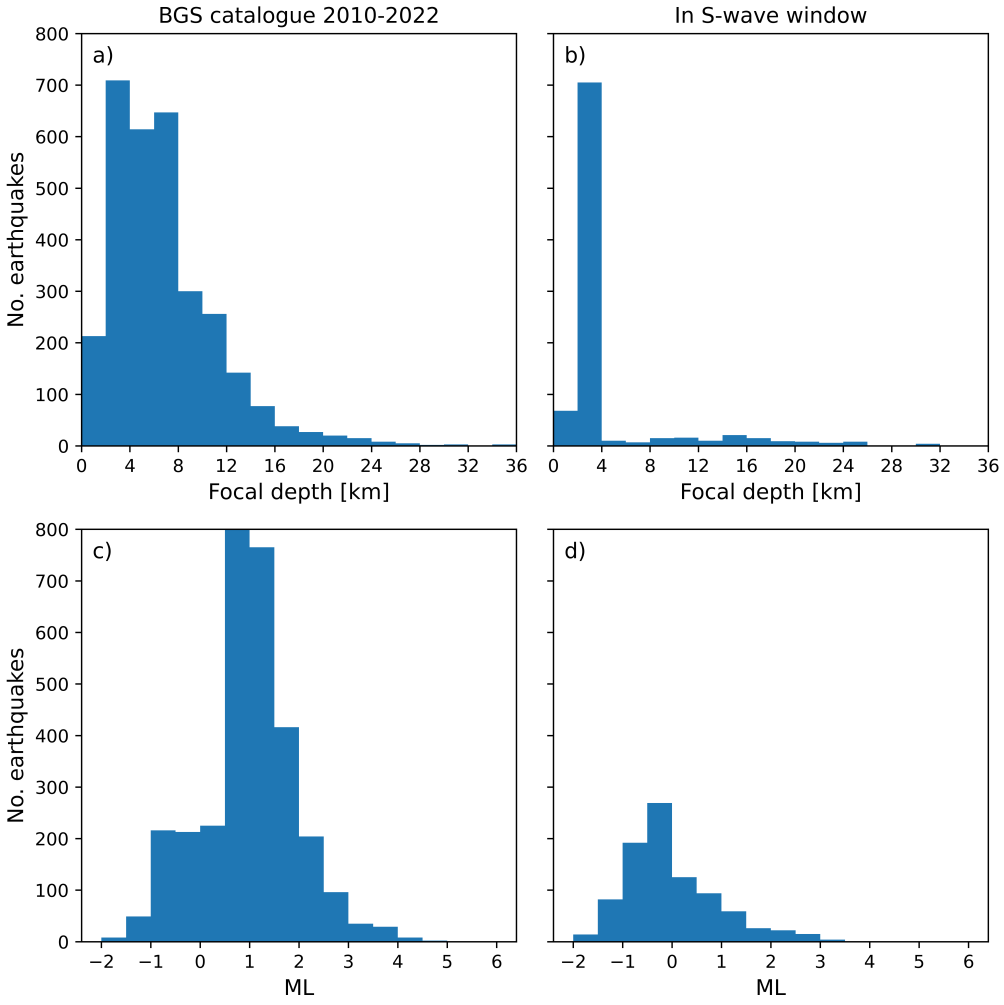

FIGURE 2: Histograms showing the focal depth (a) and local magnitude (c) of earthquakes in the British Geological Survey (BGS) catalogue for 2010 - 2022 and for the dataset of 1452 earthquakes which are viable for shear-wave splitting analysis in this report (b,,d). Note that many Preston New Road events used in this report are not reported in the BGS catalogue, which causes the spike in events with small focal depths, between 2 km – 4 km, in (b).

2.2 Offshore data

2.2.1 Skagerrak OBS

Data recorded by an five-station ocean bottom seismometer (OBS) deployment by GEUS in the Skagerrak (Figure 3) is used to attempt to assess the potential of OBS deployments to measure shear-wave splitting. Earthquake location data for 39 events detected by this OBS network was provided by GEUS. Unfortunately only 2 earthquakes have an OBS station within the shear-wave window. This limits the potential of this OBS dataset and again highlights the significant problem of the shear-wave window when attempting to retroactively use deployments to measure shear-wave splitting. OBS stations deployed close (i.e., < 1 km) to CO_2 reservoirs would not suffer this issue as the seismicity of interest (i.e., microseismicity within or close to the storage complex) would likely fall within the shear-wave window, but the shear-wave window must be taken into account when designing a monitoring network to ensure that shear-wave splitting measurements can be made for microseismic events at the reservoir depths by most stations in the network.

2.2.2 Northern North Sea PRM arrays

Permanent reservoir monitoring (PRM) systems, consisting of three-component geophones and hydrophones, have been deployed to monitor oil and gas fields in the Northern North Sea (Thompson et al., 2015). Similar PRM systems could be an option for monitoring of offshore CO_2 storage fields, but shear-wave splitting is not routinely measured for this data. PRM data for three fields in the Northern North Sea: Snorre, Grane and Oseberg, were identified as good sites to test the potential for PRM systems to measure shear-wave splitting as data from select PRM stations are shared with the Norwegian National Seismic Network (NNSN; Ottemöller et al., 2021). Of these three fields only Snorre is found to have suitable earthquakes, taken from the SHARP unified North Sea catalogue (Kettlety et al., 2024), which lie within the shear-wave window of PRM stations. These events include the 21st March 2022 M_W 5.1 Tampen Spur earthquake and six subsequent aftershocks. This initial dataset is supplemented by additional aftershocks detected using the PRM system (Jerkins et al., 2024), bringing the total dataset to 16 earthquakes with local magnitudes in the range $0.1 < M_L < 2.6$ (Figure 4). Waveform data for all earthquakes are obtained for the 10 PRM nodes shared with the NNSN and for the Tampen Spur mainshock data from an additional 50 PRM stations is provided by Equinor.

2.3 UK stress data

To benchmark the UK shear-wave splitting measurements, we use stress orientation measurements compiled by the Stress Map of Great Britain and Ireland 2022 Kingdon et al. (2022). The UK stress dataset comprises 474 data points obtains from focal mechanisms, bore breakouts, drilling induced fractures, overcoring, hydraulic fractures and geological indicators. Here we only use the 154 data points with a quality code A, B, or C (Figure 5), which indicates the data has an uncertainty in S_{Hmax} orientation of $\pm$15°, $\pm$20° or $\pm$25° respectively. To enable a consistent comparison, these quality thresholds are applied to uncertainty in fast polarisation direction when assigning quality codes to shear-wave splitting measurements.

The Stress Map of Great Britain and Ireland 2022 has few data points for the Southeastern UK (Figure 5). There are no existing data points in the Weald Basin, where we have a significant amount of seis-

micity data. To confirm the regional stress orientations borehole breakout analysis was undertaken on six boreholes in the Weald. The analysis was based on dual-caliper logs using the methodology detailed in (Heidbach et al., 2016). In total 20 breakout zones were interpreted from the six boreholes with a combined length of over 350 m.

The dominant orientation of the maximum horizontal stress is 142° with a circular standard deviation of 15°. This trend is in line with the expected regional orientation of S_{Hmax} in the UK (Kingdon et al., 2016) which have previously been attributed to ridge push in the North Atlantic (Klein and Barr, 1986). For more information on the use of calipers to determine in-situ stress orientations please see: Bell and Gough (1979), Plumb and Hickman (1985), and Heidbach et al. (2016).

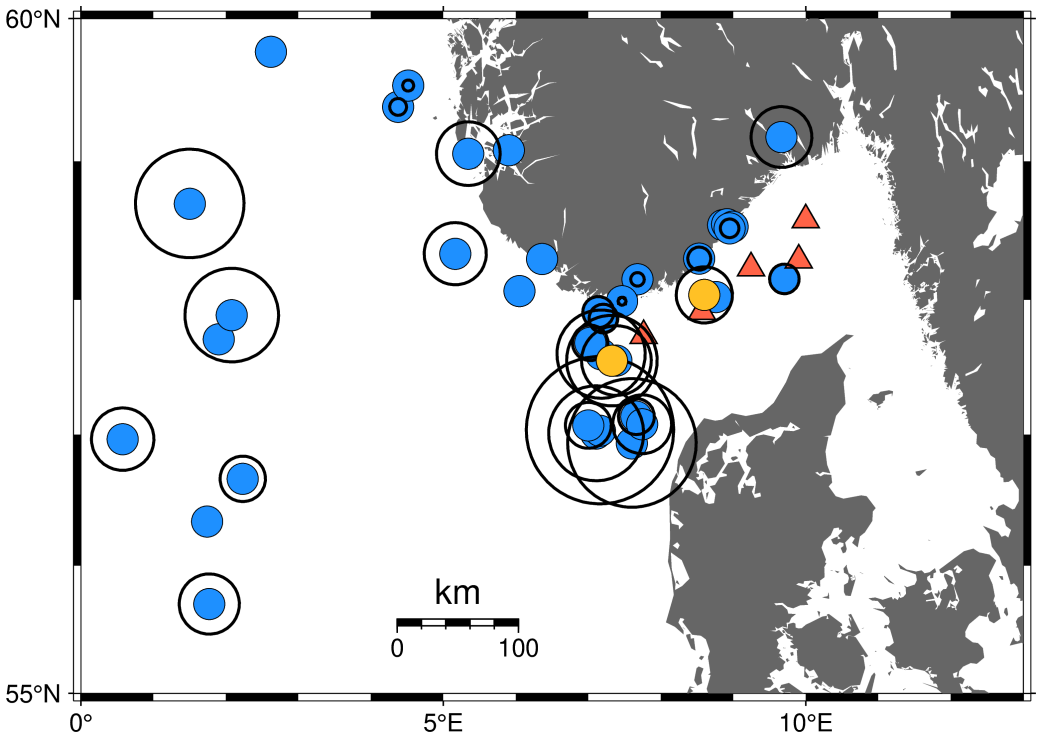

FIGURE 3: OBS stations (red triangles) and earthquakes detected by the OBS stations (blue circles) provided by GEUS. Black circles show the estimated 45° shear-wave window for each earthquake where a depth has been estimated. Earthquakes where an OBS station falls within this shear-wave window are shown in gold.

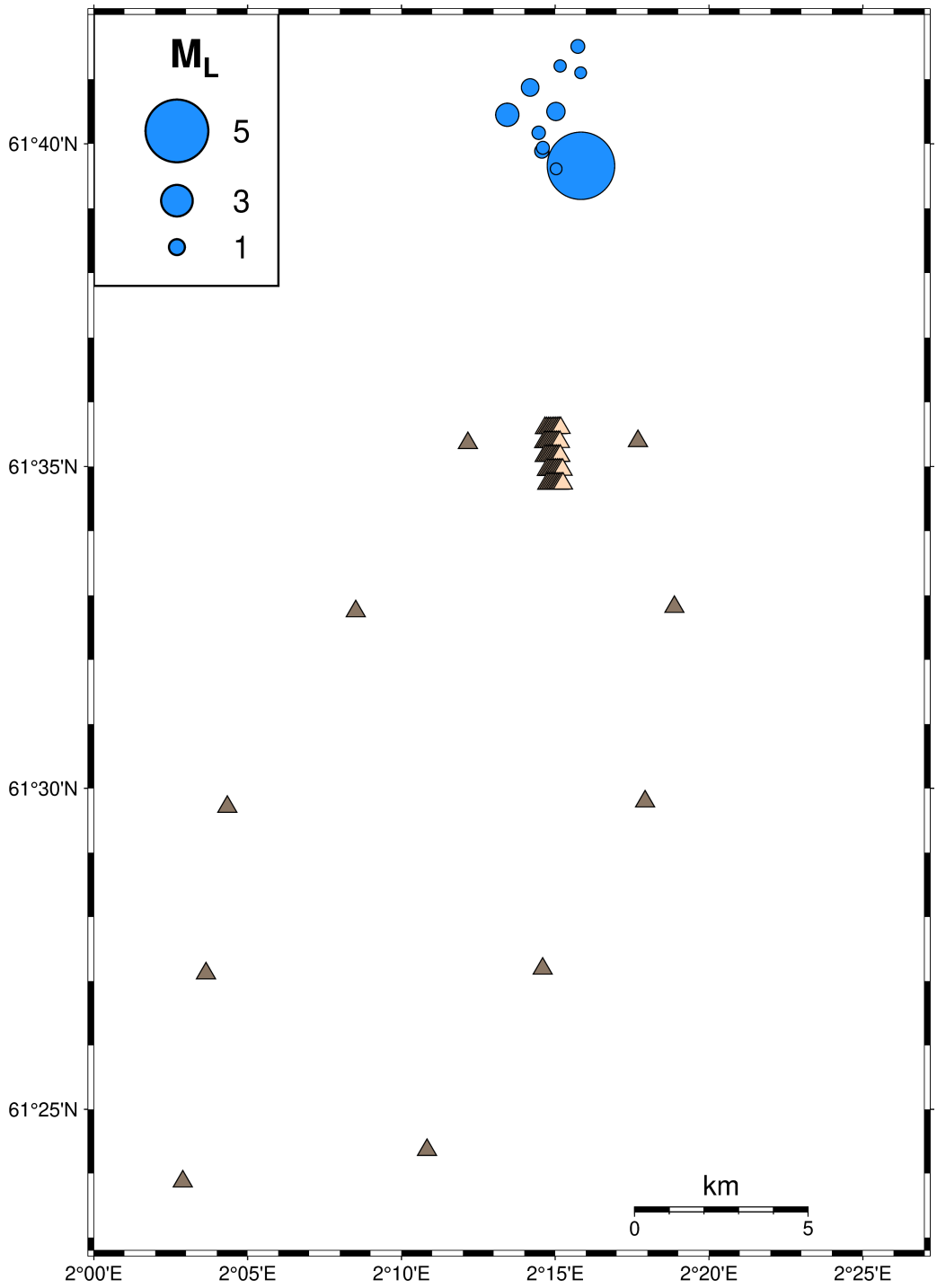

FIGURE 4: Permanent reservoir monitoring (PRM) stations (triangles) used at the Snorre field. Earthquakes used (blue circles), the 21$_{st}$ March 2022 M_W 5.1 Tampen Spur earthquake and subsequent aftershocks, are plotted at the locations of Jerkins et al. (2024). Data from 10 PRM stations, which is shared with the Norwegian National Seismic Network (Ottemöller et al., 2021), is used for all earthquakes. For the Tampen Spur mainshock, waveform data from an additional 50 PRM stations was provided by Equinor.

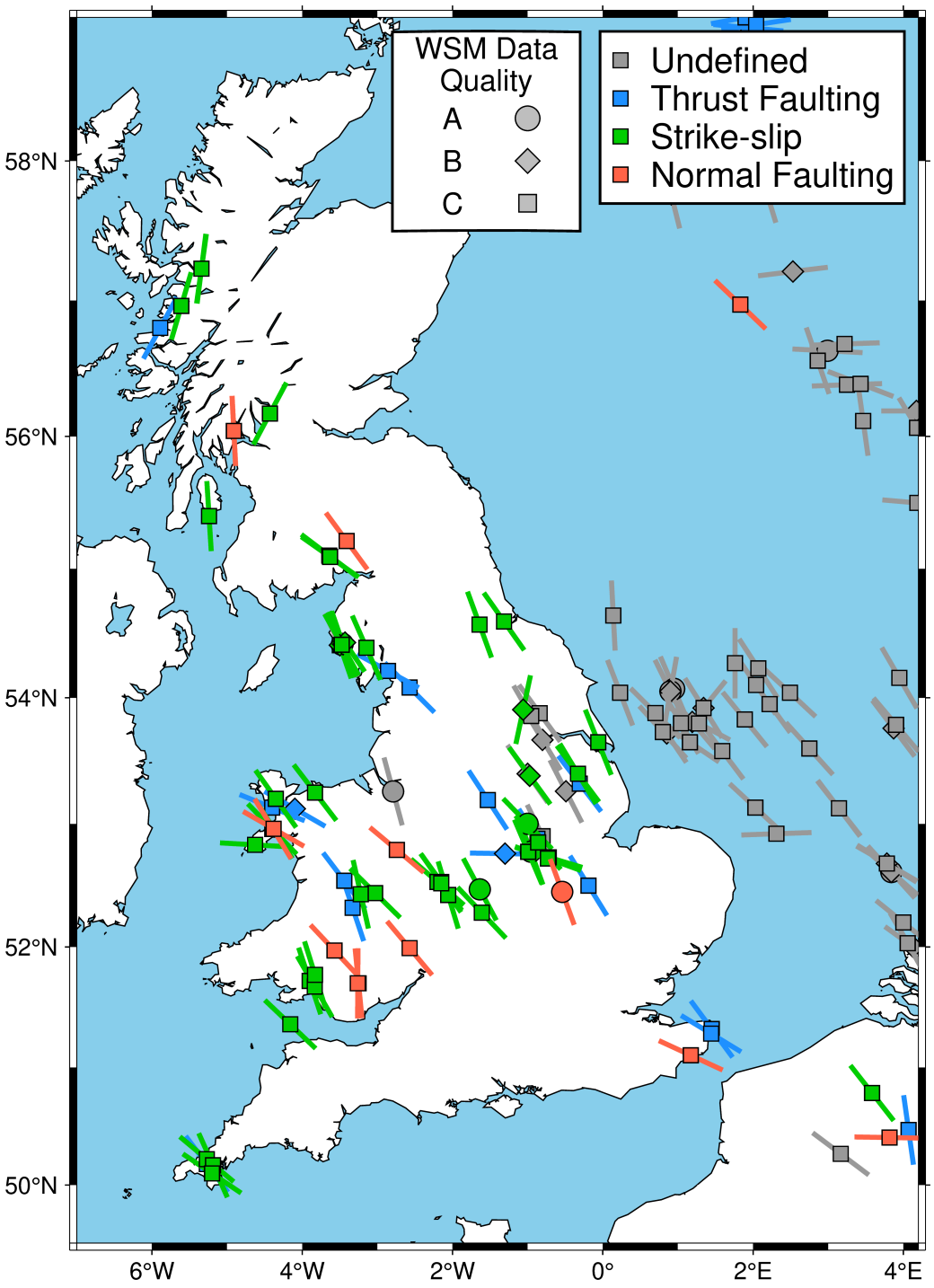

FIGURE 5: Map showing stress data with a quality of A (circle), B (diamond), or C (square) taken from the Stress Map of Great Britain and Ireland 2022 (Kingdon et al., 2022). Symbols mark the location of stress datapoints, with the bars showing the interpreted orientation of S_{Hmax}. Symbol colours indicate interpreted tectonic regime.

3 Method

When a shear-wave arrives at a station, if there has been no shear-wave splitting then the shear-wave arrival will be recorded with an approximately linear particle motion. If shear-wave splitting has occurred then the phase shift due to the delay time δt will produce an elliptical particle motion. Detecting and then correcting for this elliptical particle motion underpins most methods for measuring shear-wave splitting. Here we use eigenvalue minimisation (Silver and Chan, 1991; Walsh et al., 2013), which is widely used and robust semi-automated method for measuring shear-wave splitting. For a defined analysis window containing the shear-wave arrival of interest we grid search over a plausible range of shear-wave splitting parameters, correct for the splitting described by those parameters, and compute a trace covariance matrix, ordered such that the first and second eigenvalues represent the horizontal components. The ratios of the first and second eigenvalues describe the linearity of the particle motion, where $\lambda_2 = 0$ for linear particle motion, we seek to minimise the second eigenvalue. Uncertainties in the measured splitting parameters are estimated using the F-test

$$\lambda_2^{0.95}(\phi, \delta t) = \lambda_{2_{min}}\{1 + [k/(v-k)]F_{k,v-k}^{0.05}\}, \tag{2}$$

where $k = 2$, the number of estimated splitting parameters, v is the estimated degrees of freedom of the data and $F_{k,v-k}$ is an F-distribution (Silver and Chan, 1991; Walsh et al., 2013).

Shear-wave splitting is measured using the analysis code SHEBA (Wuestefeld et al., 2010). All waveforms are bandpass filtered between 1 Hz and 20 Hz. For each candidate event-station pair the waveforms are manually inspected and analysis window start/end ranges are picked, with cluster analysis used to pick the optimum window following Teanby et al. (2004b). Measurements are then subjected to quality control processes. Initially quality codes are assigned automatically using the estimated measurement uncertainty as follows:

- A: $\sigma_\phi \leq 15^\circ$ and $\delta t \leq 0.005\,\mathrm{s}$
- B: $\sigma_\phi \leq 20^\circ$ and $\delta t \leq 0.01\,\mathrm{s}$
- C: $\sigma_\phi \leq 25^\circ$ and $\delta t \leq 0.015\,\mathrm{s}$
- D: $\sigma_\phi \leq 40^\circ$ and $\delta t \leq 0.03\,\mathrm{s}$
- E: $\sigma_\phi > 40^\circ$ and $\delta t > 0.03\,\mathrm{s}$

Measurements are then manually inspected to validate this automatic quality control. Input waveforms, selected shear-wave window, corrected waveforms and eigenvalue minimisation surface (Figure 6) are inspected to ensure a good shear-wave splitting result has been achieved. This inspection process is important as crustal shear-wave splitting measurements commonly suffer from cycle skipping, where one shear-wave is pushed outside the measurement window, which artificially reduces the eigenvalue ratio and the estimated measurement uncertainties. Cycle skipping in shear-wave splitting measurements can be hard to detect using automated data screening methods (e.g., Savage et al., 2010a; Castellazzi et al., 2015), with manual screening being the most reliable, albeit time-consuming, way to ensure measurements effected by cycle skipping are removed. Selecting larger analysis windows can partially mitigate this issue, but then has the drawback of polluting the mea-

surement windows with additional noise or secondary arrivals. Shear-wave splitting measurements with quality codes A, B, or C are referred to as ”good“ quality.

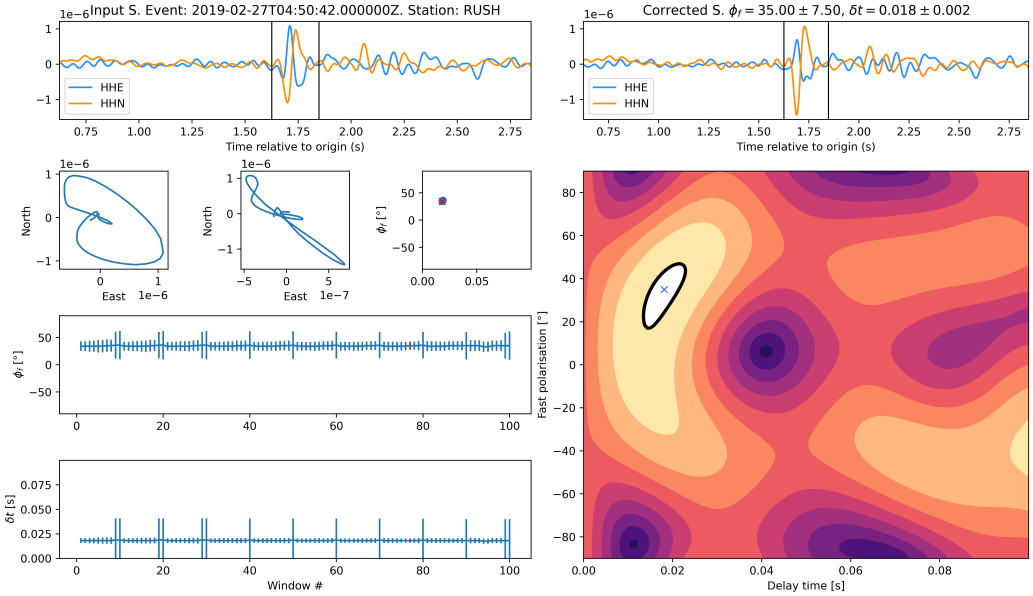

FIGURE 6: Example diagnostic output plot for a shear-wave splitting measurement made at the station RUSH for a M_L -1.1 earthquake which occurred at 2019-02-27 04:50:42 UTC. After manual inspection this measurement is categorised as an ’A’ or highest quality measurement. Top panels show the input (top left) and corrected (top right) shear-wave phase, where the vertical black bars show the optimum analysis window. The second row of the left shows the input particle motion, which is clearly elliptical, followed by the corrected, near linear, particle motion. Lower panels show ϕ_f and δt measured for each of the 100 windows used in the cluster analysis of Teanby et al. (2004b). Contour plot on the lower right shows $\frac{\lambda_2}{\lambda_1}$ calculated by the grid search. Blue cross shows the best fitting shear-wave splitting parameter, the white region enclosed by a bold black contour shows the 95% confidence region.

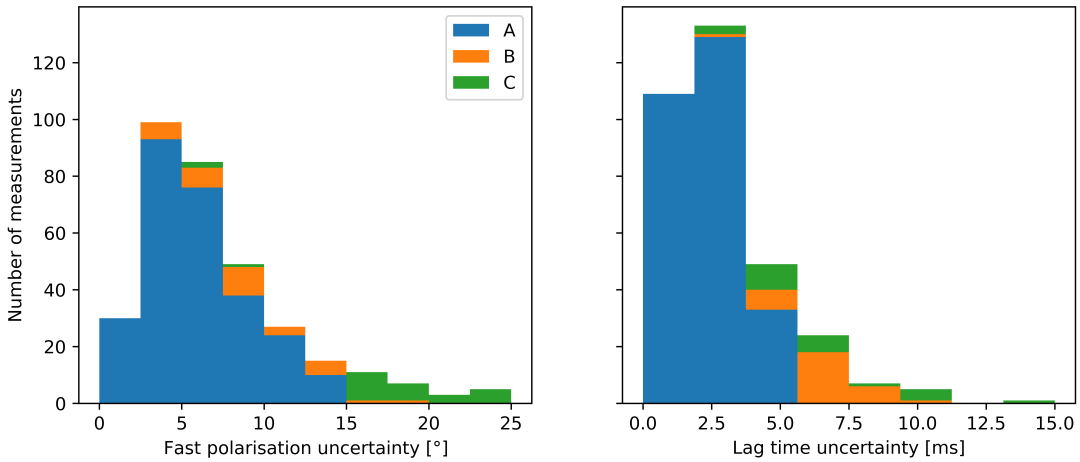

FIGURE 7: Stacked histograms of measurement uncertainties in ϕ_f (a) and δt (b) for the 329 quality A-C onshore UK shear-wave splitting measurements. See text for criteria used for different data quality codes.

4 Results

4.1 UK onshore seismicity

Shear-wave splitting is measured for all 902 candidate earthquake-station pairs, yielding 886 measurements. Measurement quality codes are assigned following uncertainty thresholds used by the World Stress Map as set out in Chapter 3. We will only use the 329 measurements that are quality A-C for further analysis in this report. The uncertainties in ϕ_f and δt (Figure 7) are such that where we have good quality shear-wave splitting measurements we can confidently constraint potential S_{Hmax} orientations and resolve spatiotemporal variation in shear-wave splitting.

Data attrition is primarily due to noisy data producing measurements with large uncertainties, cycle skipping, and null measurements. Null shear-wave splitting measurements (i.e., where no splitting is observed) can be useful data points in some scenarios and occur either if there is no anisotropic medium, the shear-wave source polarisation closely aligns with the fast polarisation direction, or if there are multiple layers of anisotropy which align such that the apparent splitting is null. In the context of constraining crustal stress, none of these cases are particularly useful and the 50 null measurements are removed. In a monitoring scenario including null measurements could be useful, as stress changes in the caprock that induce a change in seismic anisotropy could cause a temporal change in shear-wave splitting where null measurements sampling a section of the caprock become splits, or vice-versa.

Comparing the shear-wave splitting measurements to stress data from the Stress Map of Great Britain and Ireland (Figure 8) shows that there are few regions where we can make a good comparison to the existing stress data due to the geographical heterogeneity introduced by the shear-wave window limitation and the coverage of the stress data, which is lacking in Southern England. There are four regions where we can make good comparisons between World Stress map data:

1. Northwest England
2. Northeast England
3. South Wales
4. Southeast England

These regions are indicated by the corresponding numbers in Figure 8. The latter two of these regions are represented by localities: Preston New Road, Lancashire, and Newdigate, Surrey. These localities have dense shear-wave splitting datasets which enable more detailed analysis.

4.1.1 Northeast England

There are 9 quality A-C measurements of shear-wave splitting in this region (Figure 9), measured for earthquakes with depths ranging from 9.6 km to 31.4 km and local magnitudes in the range $1.2 \leq M_L \leq 2.6$. This limited dataset limits the scope for any detailed interpretation. The stress data shows a NW-SE regional trend, with one quality B data point showing a North-South S_{Hmax} orientation. Five shear-wave splitting fast polarisation measurements show some agreement with the regional stress field, within the 25° uncertainty of the quality C stress data, with the other measurements showing contradictory orientations. These disagreeing data points suggest that there could be some local heterogeneity in the seismic anisotropy, but with such a sparse data set it is difficult to interpret what the source of this variation in seismic anisotropy may be.

4.1.2 South Wales

In South Wales we make 19 measurements of shear-wave splitting (Figure 10) for earthquakes with depths in the range 10 km - 25.6 km and local magnitudes in the range $0.5 \leq M_L \leq 2.7$. As for North East England, we observe some scatter in the shear-wave splitting fast polarisation measurements. Seven measurement agrees show agreement with the regional orientation of S_{Hmax}, within the 25 degree uncertainty of the quality C data points in the region (Figure 11). One possible explanation for the variation in shear-wave splitting measurements could be multiple layers of anisotropy, with shear-waves from deeper earthquakes sampling multiple anisotropic media along their ray path. Plotting the South Wales shear-wave splitting measurements as a function of depth does not show any significant variation in % anisotropy with depth (Figure 11). We convert splitting delay times δt to percent anisotropy ξ to remove dependence of delay times on ray path length d following

$$\xi = 100(V_S * \frac{\delta t}{d}),$$

where V_S is the regional mean shear-wave velocity which is assumed to be 3 km s^{-1}. Figure 11 shows all fast polarisation measurements with focal depths > 18 km deviate from the regional S_{Hmax}, therefore it possible that there is a second layer of anisotropy at depth. The shallower scatter in fast polar-

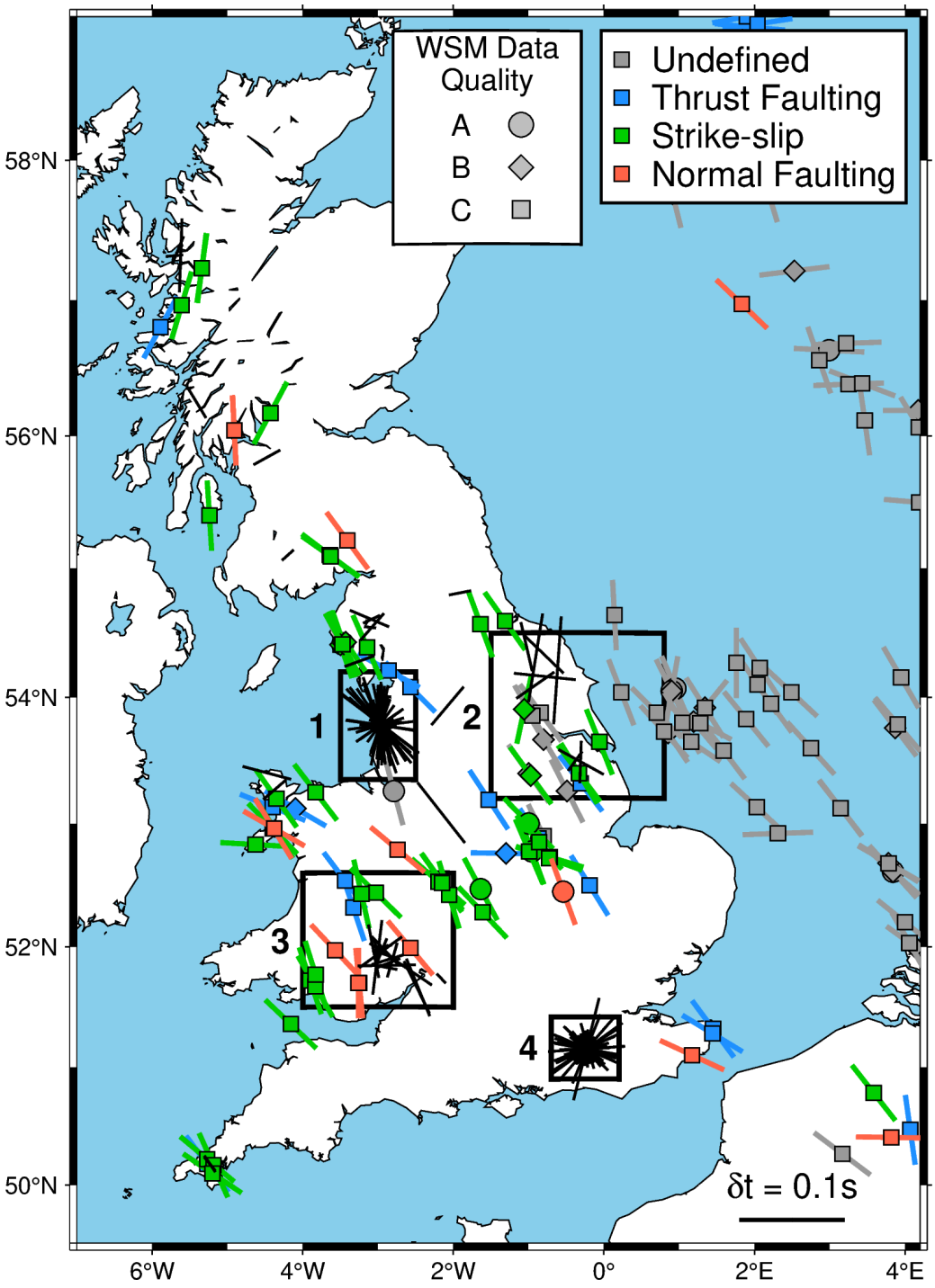

FIGURE 8: Map showing the 329 quality A-C shear-wave splitting measurements, overlain on quality A-C stress measurements taken from the Stress Map of Great Britain and Ireland (Kingdon et al., 2022). Shear-wave splitting measurements are plotted as bars located at the earthquake-station midpoint where the bar orientation shows the measured fast polarisation direction and bar length is proportional to δt. Stress data are plotted following Figure 5. Regions where comparison between shear-wave splitting measurements and World Stress Map data can be made are shown in boxes. The regions are; Northwest England (1), Northeast England (2), South Wales (3), and Southeast England (4).

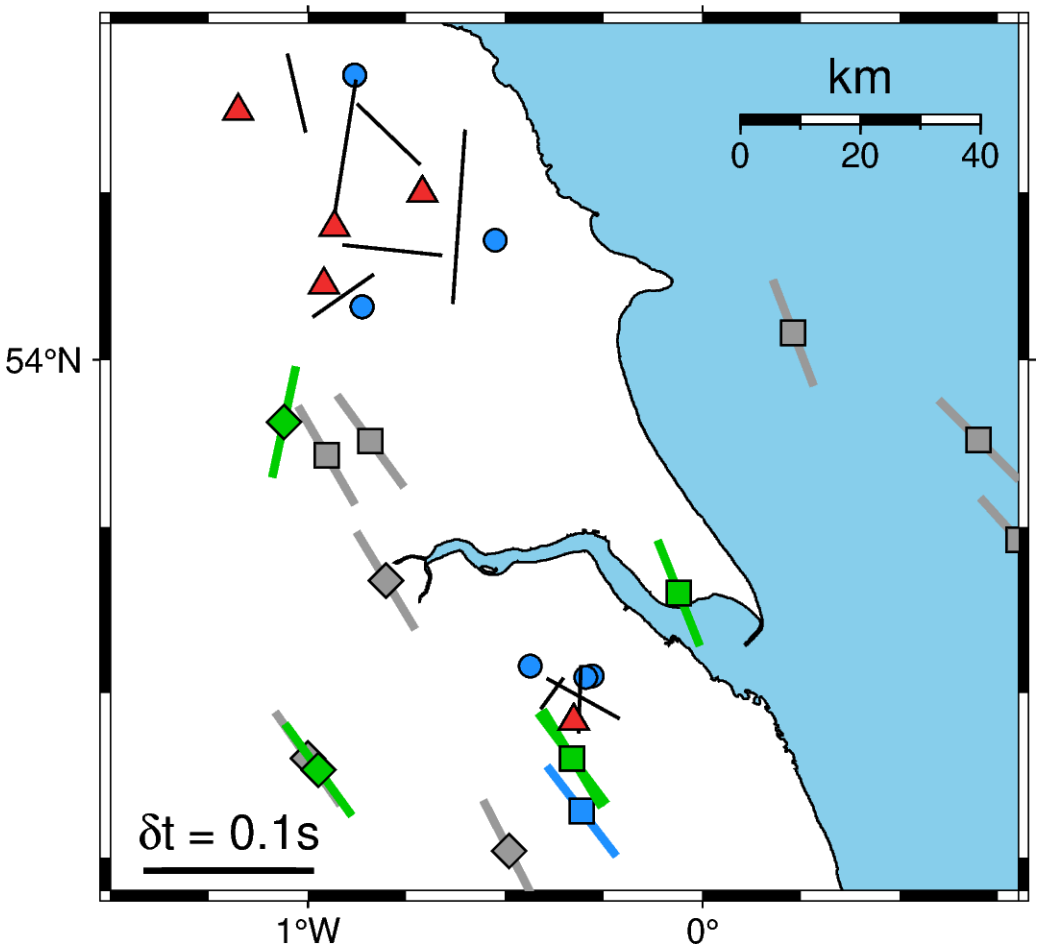

FIGURE 9: Map showing shear-wave splitting results for North East England and stress data taken from the Stress Map of Great Britain and Ireland (Kingdon et al., 2022). Shear-wave splitting measurements are plotted as bars located at the earthquake-station midpoint where the bar orientation shows the measured fast polarisation direction and bar length is proportional to δt. Stress data are plotted following Figure 5.

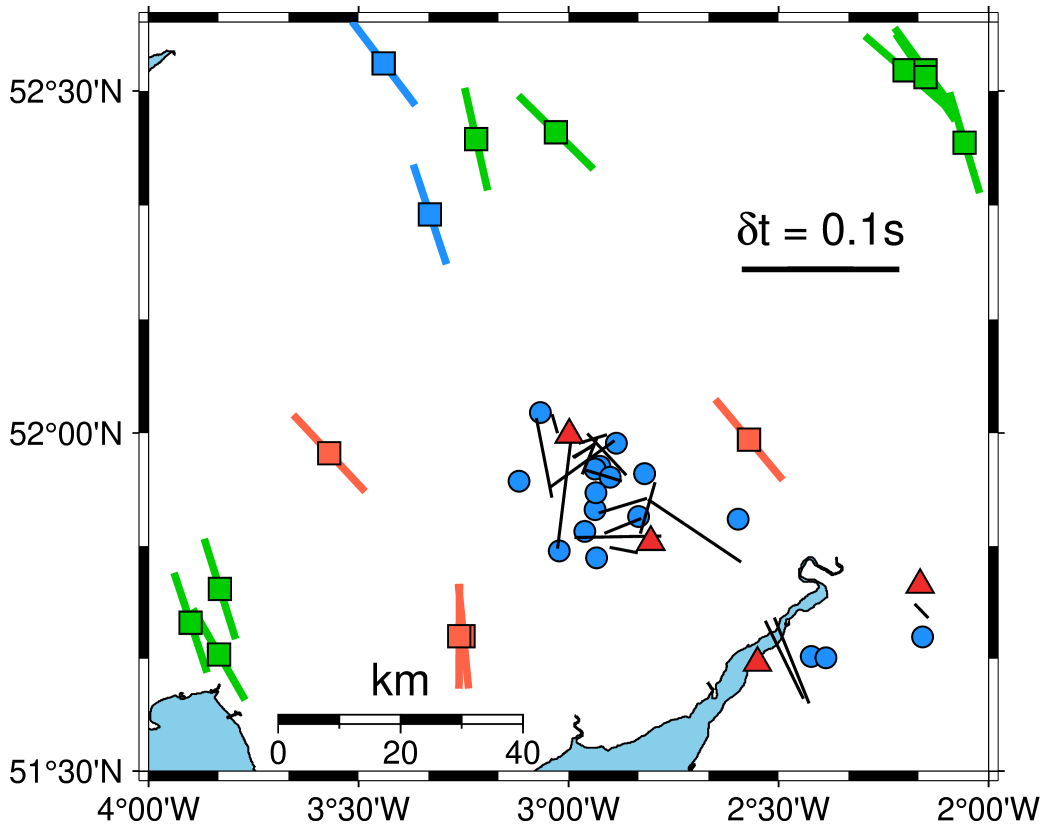

FIGURE 10: Map showing shear-wave splitting results for South West Wales and stress data taken from the Stress Map of Great Britain and Ireland (Kingdon et al., 2022). Shear-wave splitting measurements are plotted as bars located at the earthquake-station midpoint where the bar orientation shows the measured fast polarisation direction and bar length is proportional to δt. Stress data are plotted following Figure 5.

isation measurements could again be explained by heterogeneous anisotropy, where the observed seismic anisotropy varies with azimuth at the station, particularly as the discordant measurements are all made for the central earthquake cluster with three fast polarisation measurements recorded in the South East of the region agreeing with S_{Hmax}.

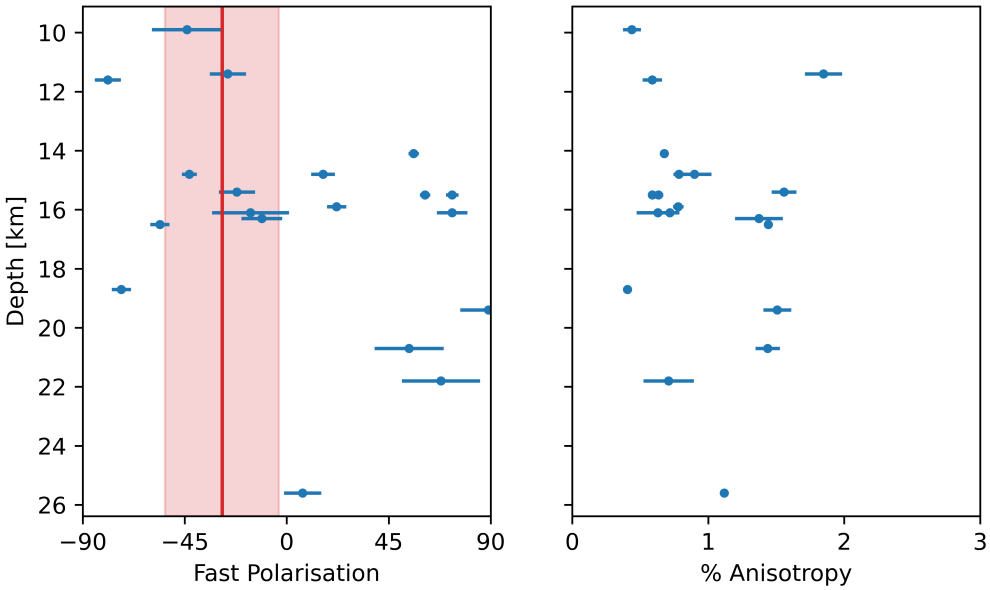

FIGURE 11: Histograms showing measured shear-wave splitting for South Wales as a function of depth. To reduced dependency of variance in ray path length d, shear-wave splitting delay times are converted to % anisotropy ξ following $\xi = 100 * (V_S * \delta t/d)$ where V_S is the regional mean shear-wave velocity, assumed to be 3 km s^{-1}. Red bar shows the circular mean S_{Hmax} orientation for South Wales with the shaded region representing the 25° uncertainty in quality C stress data.

4.1.3 Preston New Road

In 2018 and 2019, hydraulic fracturing took place on two horizontal wells drilled in Northwest England. This was the "Preston New Road" shale gas project, operated by Cuadrilla Resources Limited, which was located around 3 km east of the town of Blackpool. Shortly before, during, and for some months after injection, microseismic monitoring was conducted by the operator. Independent monitoring was also done by the British Geological Survey. The surface arrays of three-component short period and broadband sensors recorded hundreds of events in the two periods of hydraulic fracturing. A small number of events were felt by nearby populations. This felt induced seismicity, along with other external political pressures, eventually led to a moratorium on hydraulic fracturing in England. It should be noted that whilst the names of seismic stations changed between the two stages of injection, the locations and type of sensors at each location remained consistent. The continuous waveform data from this monitoring effort have since been made publicly available for study.

We make 180 shear-wave splitting measurements for stations at Preston New Road for earthquakes with depths ranging from 1.6 km to 2.9 km and local magnitudes in the range $-1.7 \leq M_L \leq 2.9$. Of these, 115 are made using events detected during the first stage of hydraulic fracturing (in 2018, Figure 12) and 65 are made for events occurring during the second stage (in 2019, Figure 13). At Preston New Road, we are able to directly compare our measured shear-wave splitting fast polarisation directions with stress data interpreted from analysis of borehole breakout and drilling induced tensile fractures for a borehole drilling nearby at Preese Hall (PH-1), which gives interprets a regional S_{Hmax} orientation

of 173 ± 7° (Figure 12, 13; Clarke et al., 2019a).

Shear-wave splitting fast polarisation directions, for stations with 10 or more measurements, show good agreement with the interpreted S_{Hmax} (Figure 14). This suggest that for the shallow (< ca. 2 km) seismicity at Preston New Road, stress induced alignment of sub-vertical cracks can explain the observed shear-wave splitting. At station AQ04, there are possible signs of small scale rotation in S_{Hmax}, but this is within the measurement uncertainty of the PH-1 data. Station IO1 shows a second modal fast polarisation direction rotated approximately 30° from S_{Hmax}. When the splitting results are plotted at their ray midpoint, an approximation of the location of the anisotropic medium, these results do not form one clear cluster, which would indicate path effect effects, and are instead spread across the space sampled by IO1. This suggested the presence of a second, conjugate set of cracks as a plausible explanation for the bimodal fast polarisation directions. A more optimally deployed set of sensors, to increase azimuthal coverage, would enable better characterisation of settings with multiple fracture sets.

As the hydraulic fracturing at Preston New road was done to two discrete stages, separated in time, we can attempt to search for signatures of temporally-varying shear-wave splitting. A temporal change in shear-wave splitting, if observed, could reflect a change in overburden stress. Time varying signatures in anisotropy have been associated with stress changes due to crustal processes (e.g., Crampin et al., 1999; Liu et al., 2014). Alternatively a change in anisotropy could represent a change in fracture properties such as fracture density, length, or aspect ratio. At Preston New Road, the seismic station locations remain constant but the station names are changed from IOXX to PNRXX. Shear-wave splitting for eastward propagating raypaths, recorded at IO2 and PNR02 do not exhibit any signs of temporal variation and show very stable fast polarisation directions (Figure 14). It is unclear if there is any temporal variation between IO1 and PNR01 (Figure 15) as less data are recorded at PNR01, with the 15 measurements at PNR01 preferentially sampling the secondary fracture set. At IO3B and PNR3B there a stronger signature of a change in anisotropy. These stations again appear to see two fracture sets, with the orientation of the secondary cracks fractures changing from Stage 1 to Stage 2. However, the number of measurements is too small to be confident a temporal signature in the shear-wave splitting is observed.

4.1.4 Newdigate, Surrey

In 2018-9 an earthquake swarm occurred in Southeast England near Newdigate, Surrey. Initially attributed to industrial activities nearby, it was quickly shown to be a natural earthquake swarm associated with tectonic reactivation along a pre-existing E-W striking fault in the Weald Basin (Hicks et al., 2019). We are able to make 108 quality A-C shear-wave splitting measurements for this shallow earthquake swarm (Figure 16), with focal depths ranging from 2 km to 3.6 km and local magnitudes in the range $-1.6 \leq M_L \leq 3.1$ (Hicks et al., 2019). The majority of the data is concentrated at two stations: RUSH and STAN. This is due to the tight shear-wave window constraints imposed by the shallow earthquake depths, with most swarm having a focal depth $< 2.3\,\mathrm{km}$. This region had no existing stress data, so we collect new borehole stress measurements interpreted from borehole breakouts across the Weald basin (Figure 17), which give an average regional S_{Hmax} of 142° with a circular standard deviation of 15°.

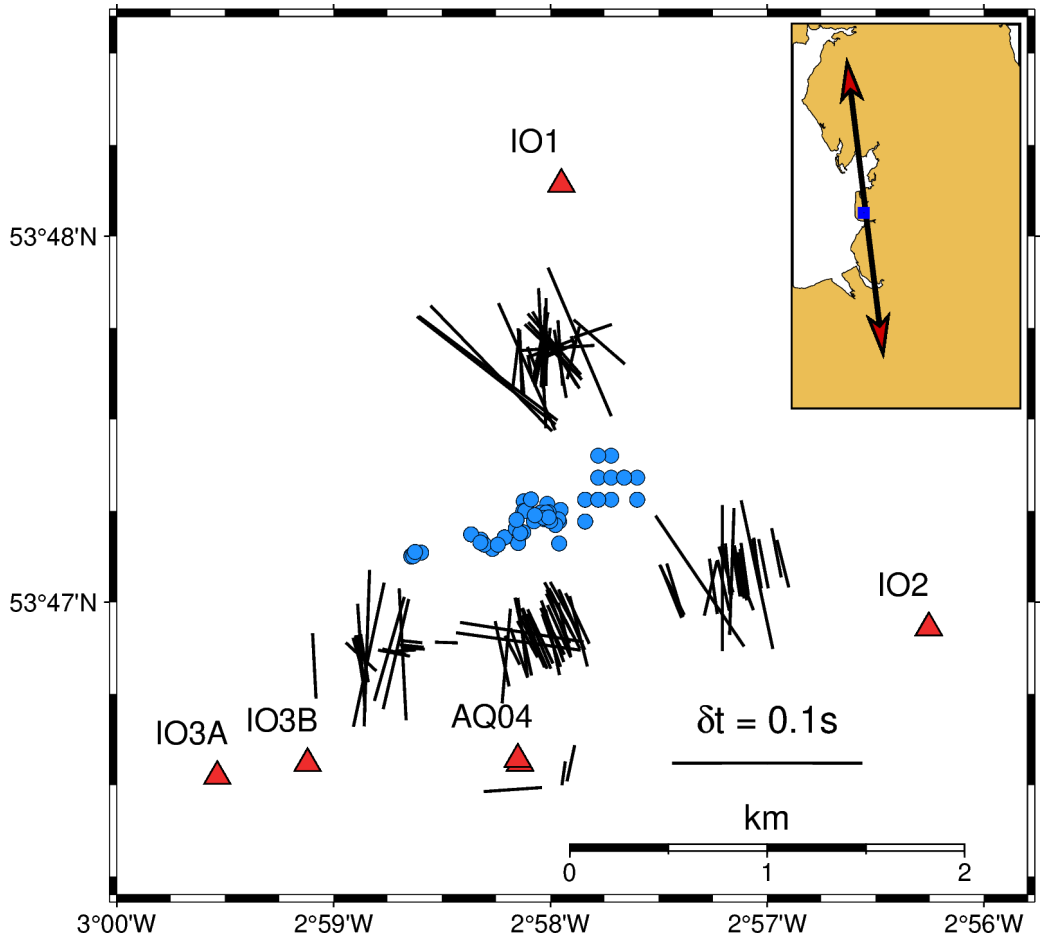

FIGURE 12: Map showing all good quality shear-wave splitting measurements for Preston New Road Stage 1. Earthquake locations are shown by the blue circles, with stations shown by the red triangles. Shear-wave splitting plotted at the ray mid-point as black bars where the bar orientation shows ϕ_f and bar length is proportional to δt. Inset map shows location of Preston New Road in the North West England and the S_{Hmax} measured by Clarke et al. (2019a) at Preese Hall 1.

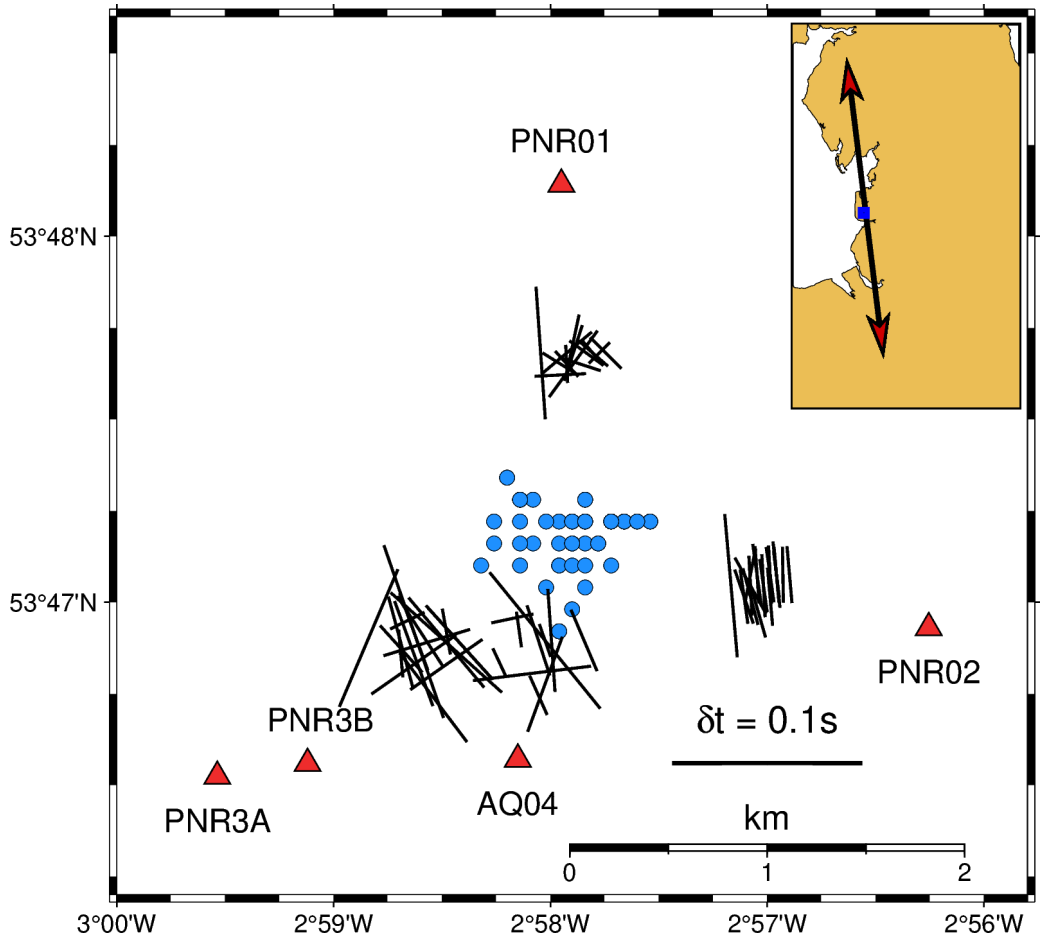

FIGURE 13: Map showing all good quality shear-wave splitting measurements for Preston New Road Stage 2. Earthquake locations are shown by the blue circles, with stations shown by the red triangles. Shear-wave splitting plotted at the ray mid-point as black bars where the bar orientation shows ϕ_f and bar length is proportional to δt. Inset map shows location of Preston New Road in the North West England and the S_{Hmax} measured by Clarke et al. (2019a) at Preese Hall 1.

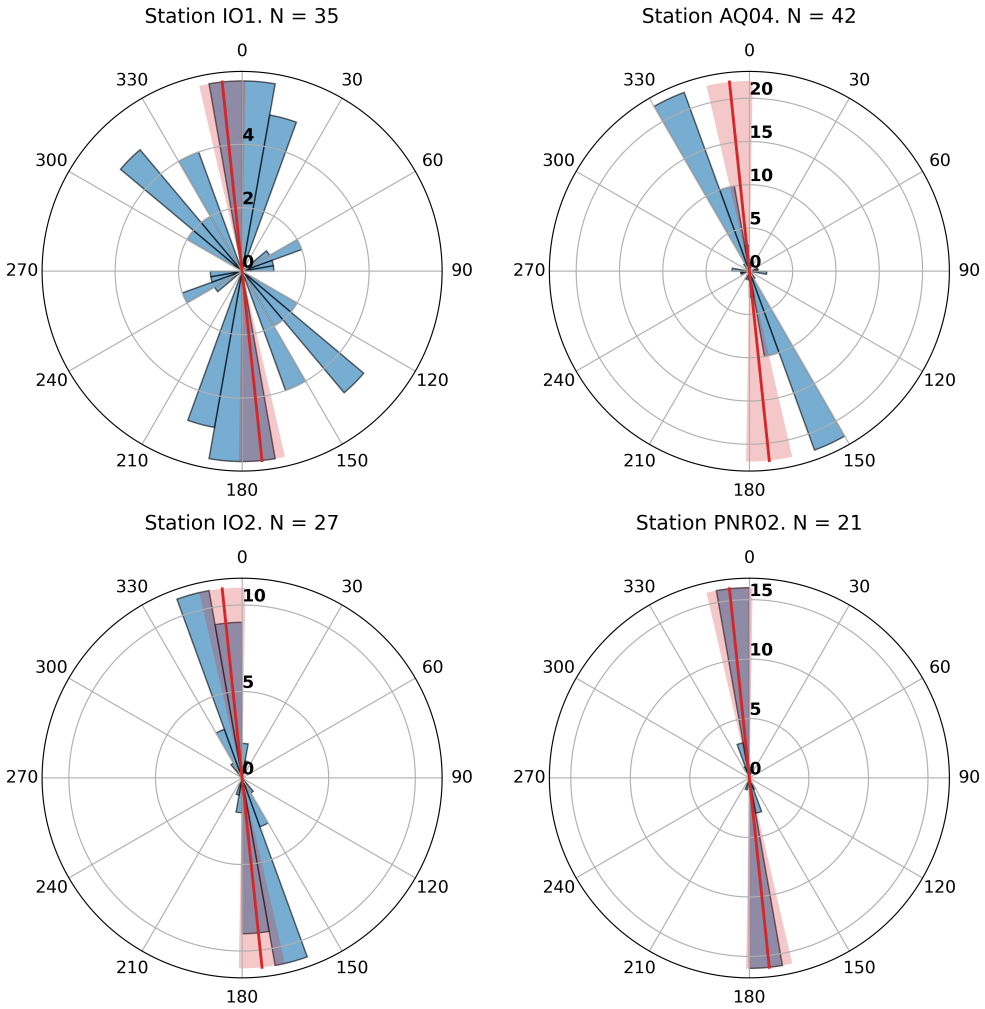

FIGURE 14: Rose histograms of fast polarisation directions measured at stations at Preston New Road, Lancashire. Red line show the local S_{Hmax} interpreted by Clarke et al. (2019a), with the red shaded region shows the measurement uncertainty. Stations IO2 and PNR02 are co-located, with the station codes changing from Stage 1 to Stage 2 injection.

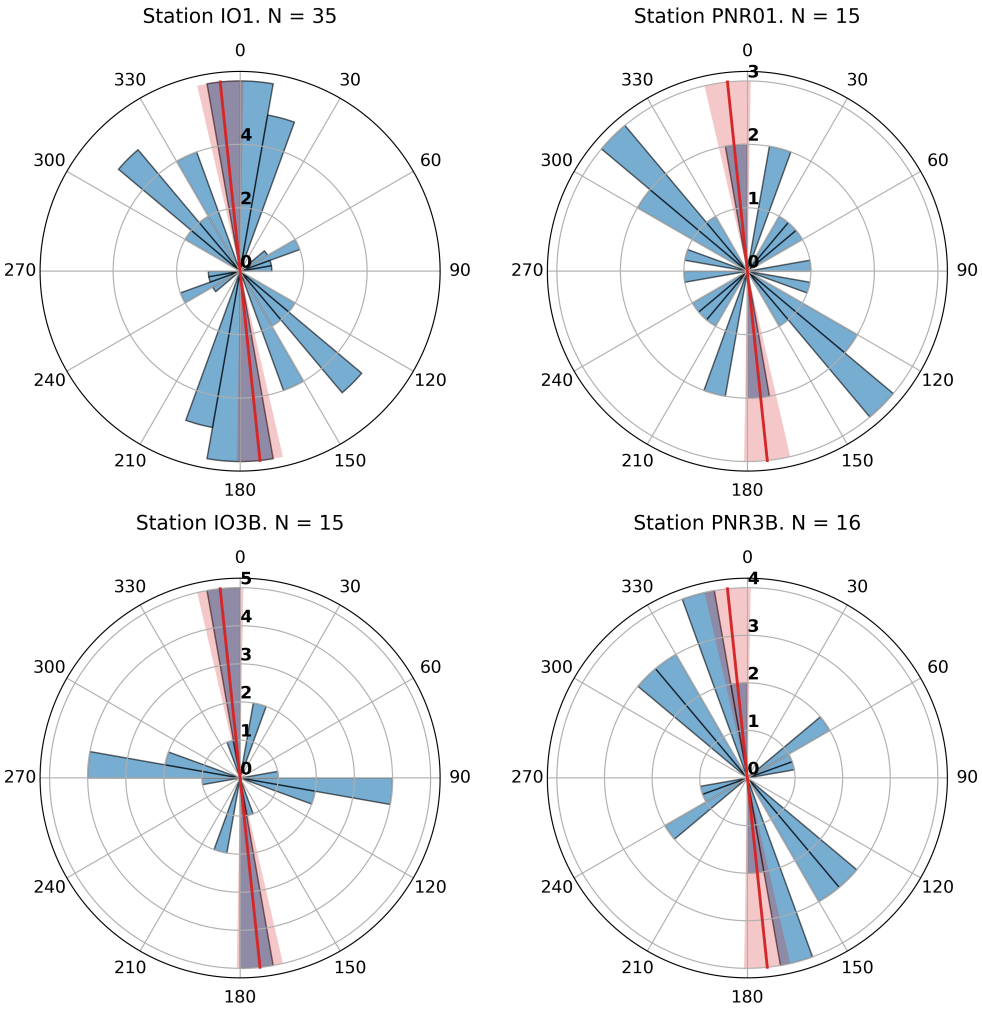

FIGURE 15: Rose histograms of fast polarisation directions measured at two stations during Stage 1 and Stage 2 injection at Preston New Road, Lancashire. Stations IO1/PNR01 (top row) and IO3B/PNR3B (bottom row) are co-located. Red line show the local S_{Hmax} interpreted by Clarke et al. (2019a), with the red shaded region shows the measurement uncertainty.

The fast polarisation directions measured at RUSH and STAN are sub-perpendicular (Figure 19). Plotting the shear-wave splitting results at the ray midpoint, which approximates the location of anisotropy, shows a change in fast polarisation directions between measurements North of the earthquake swarm (primarily recorded at STAN) and those to the South (primarily recorded at RUSH). The stations RUSH and STAN lie either side of the E-W striking fault which reactivated during the earthquake swarm, so these initially contradictory fast polarisation measurements could represent different stress conditions on either side of the fault. The fast polarisation directions seen at STAN (Figure 19, bottom panel), are rotated approximately 30° from this regional average suggesting a slight local rotation in S_{Hmax} which is within the range of borehole breakout measurements (Figure 17). Fewer measurements are made at GAT2, GATW, HORS and BRDL due to the shear-wave window limitation (Hicks et al., 2019) but these measurements support the trend observed at RUSH and STAN (Figure 16). Interestingly the stations GATW and GAT2, which are located close together (< ca. 100 m), show fast polarisation directions that agree with RUSH and STAN respectively. The shear-wave splitting measurements at GATW and GAT2 suggest there may be a temporal variation in shear-wave splitting, as the station GATW was decommissioned before GAT2 was installed. Several previous studies have observed temporal changes in shear-wave splitting associated with stress changes due to volcanic eruptions (e.g., Savage et al., 2010a; Kendall et al., 2024, in revision), earthquakes (Volti and Crampin, 2003) and petroleum extraction (Teanby et al., 2004a). In particular Savage et al. (2010a) and Teanby et al. (2004a) observe near 90° rotation in fast polarisation directions. At Newdigate we observe slightly different behaviour (Figure 18). As the earthquake swarm progresses % anisotropy markedly increases at RUSH following the July 18th 2018 M_L 2.4 earthquake and then again following the February 27th 2019 M_L 3.2 earthquake before gradually decreasing. Whilst the fast polarisation at RUSH is generally unchanged over time, at STAN we see the majority of deviations away from regional S_{Hmax} occur immediately before or following the M_L 3.2 event and when % anisotropy is elevated. For GATW and GAT2, the change in fast polarisation direction coincides with a reduction in % anisotropy, with fast polarisation returning to align with regional S_{Hmax} as the swarm subsides. These changes in anisotropy could represent local stress changes during the earthquake swarm followed by the stress state returning to follow the regional stress field.

Without *in situ* measurements South of the Newdigate fault, we cannot be certain that we are observing a change in stress state between the northern and southern fault blocks. As the data recorded at RUSH is in a limited azimuthal range, it is possible we are observing local heterogeneities in seismic anisotropy. However, local heterogeneity would not explain the clear temporal variation in % anisotropy during the Newdigate sequence. This change in anisotropy is best explained by an increase in stress, which dilates and preferentially aligns cracks, followed by a stress release during the earthquake swarm. Similar temporal variations in anisotropy have been observed during earthquake sequences in Iceland (Volti and Crampin, 2003). These interesting results highlight the potential for seismic anisotropy to observed local-scale changes in the state of stress and S_{Hmax} orientation in the subsurface. It also highlights the interpretation challenges. In hindsight additional monitoring stations could have been deployed during the Newdigate sequence, particularly to the South of the Newdigate fault where the additional data at a different azimuth would significantly strengthen out hypothesis that the change in shear-wave splitting fast polarisation directions represent a change

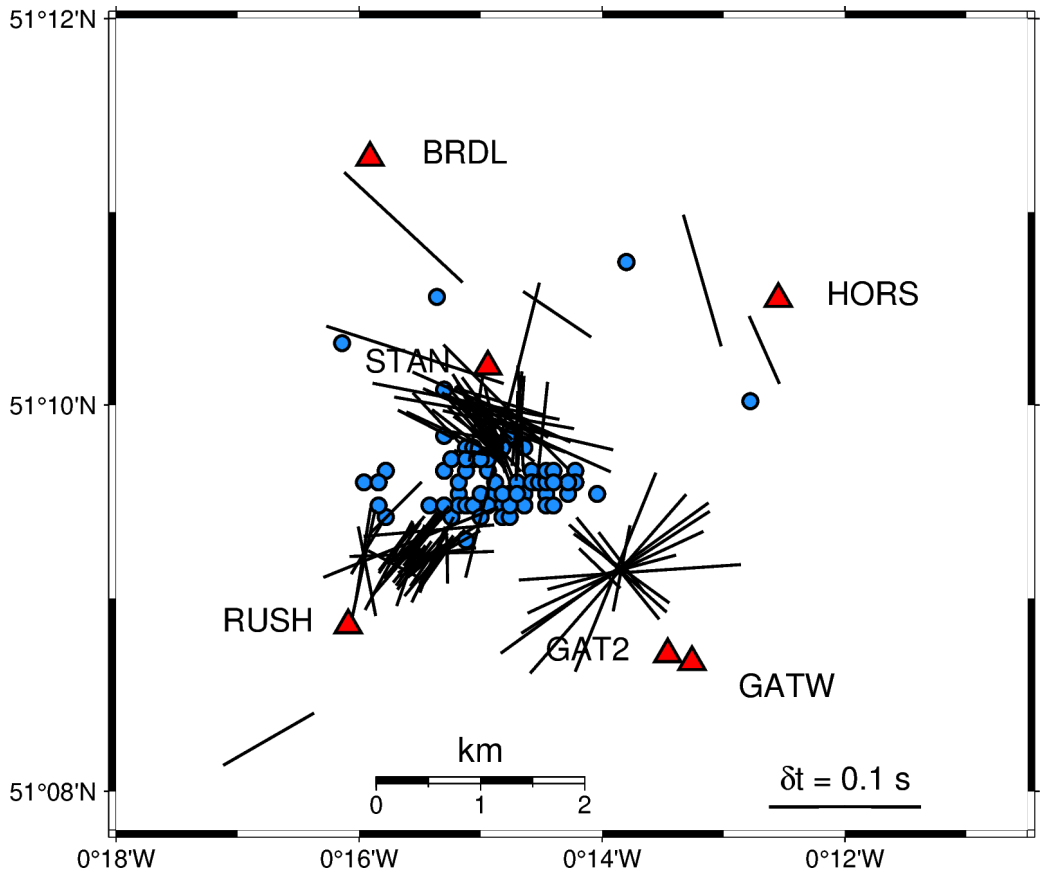

FIGURE 16: Map of shear-wave splitting measurements for Newdigate, Surrey. Measurements are plotted following the conventions in Figure 12. Inset map shows new interpretations of S_{Hmax} across the Weald basin from historic borehole logs.

in stress across the Newdigate fault. For onshore monitoring instrumentation advances may make this feasible at reasonably low cost, with seismic nodes being shown to have good potential to measure shear-wave splitting when arranged to form an effective 3-component instrument (Hudson et al., 2024). For offshore CO_2 monitoring where, unlike Newdigate, the subsurface is well-characterised, there will be more contextualising data available to assist interpretations of shear-wave splitting measurements.

4.2 Offshore data

For the 16 usable earthquakes recorded by Permanent Reservoir Monitoring stations at Snorre we make 125 measurements of shear-wave splitting, of which 34 have quality codes A-C. As for the onshore data, cycle skipping reduces the number of usable measurements. We also find that the majority of data recorded for the Tampen Spur mainshock do not yield usable shear-wave splitting measurements. This is due to data clipping on the NNSN sensors and ringing on the additional 50, unclipped, sensors provided by Equinor. The aftershock sequences generally yield clear waveforms with a good signal-to-noise ratio.

Data from across the Northern North Sea, taken from the World Stress Map 2016 release (Heidbach et al., 2016; Heidbach et al., 2018), indicates a regional S_{Hmax} which is approximately oriented East-West (Figure 20). Unlike the onshore UK results, no PRM station has enough shear-wave splitting

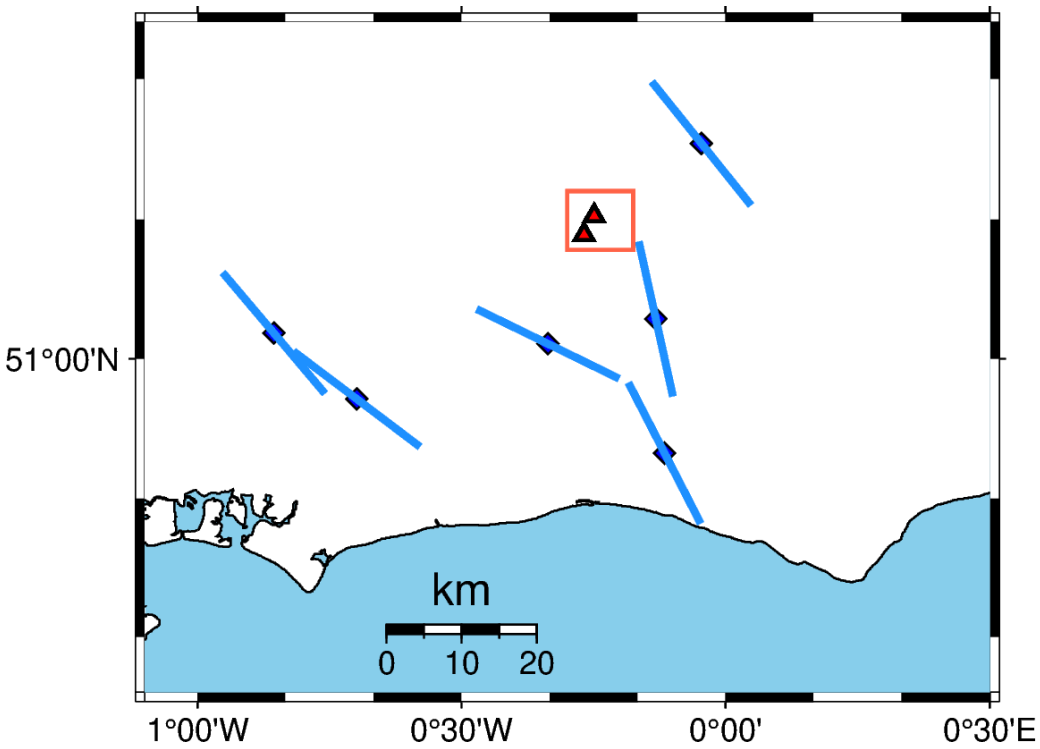

FIGURE 17: Map showing the new regional stress orientations interpreted for 6 boreholes across the Weald basin. Bar orientation shows interpreted S_{Hmax} orientation. Red box shows extent of Figure 16.

measurements for a meaningful rose histogram to be made. However, the station density does allow for some trends to be picked out. The shear-wave splitting measurements for Snorre, when plotted at the ray midpoint (i.e, half-way along the ray path between the earthquake and the station; Figure 21), the shear-wave splitting fast polarisation directions broadly align with the East-West S_{Hmax} orientation. There is some local scatter, which is similar to what we observed in the onshore UK data. These results show that offshore monitoring systems can make high-quality measurements on shear-wave splitting for microseismicity. The measurements for Snorre show that S_{Hmax} to the North of the field is aligned with the regional stress field following the March 2022 M_W 5.1 Tampen Spur earthquake.

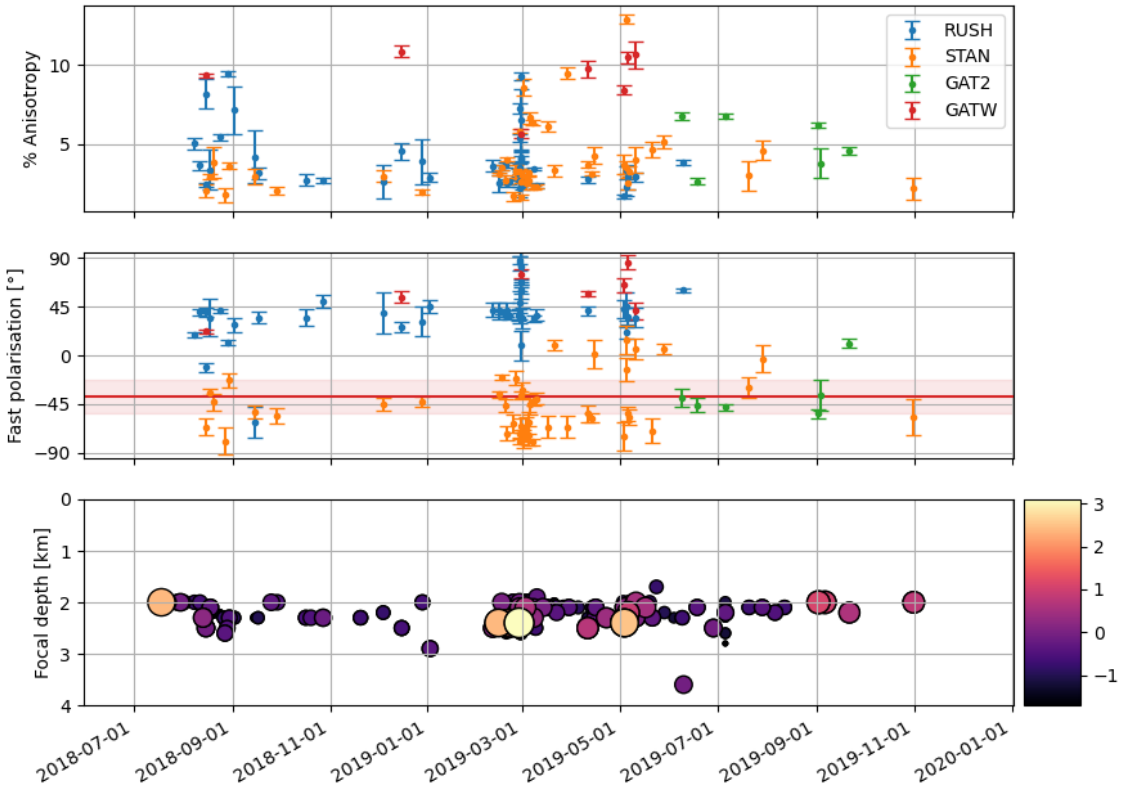

FIGURE 18: Measured shear-wave splitting for the Newdigate sequence plotted at corresponding earthquake origin times. Top panel shows temporal variations in % anisotropy. Middle panel shows changes in fast polarisation direction, where the red bar represents the regional mean S_{Hmax} of 142° and the shaded region the circular standard deviation of 15°. Bottom panel shows the focal depths of the Newdigate Earthquake swarm over time, where the circle size and colour is scaled by local magnitude.

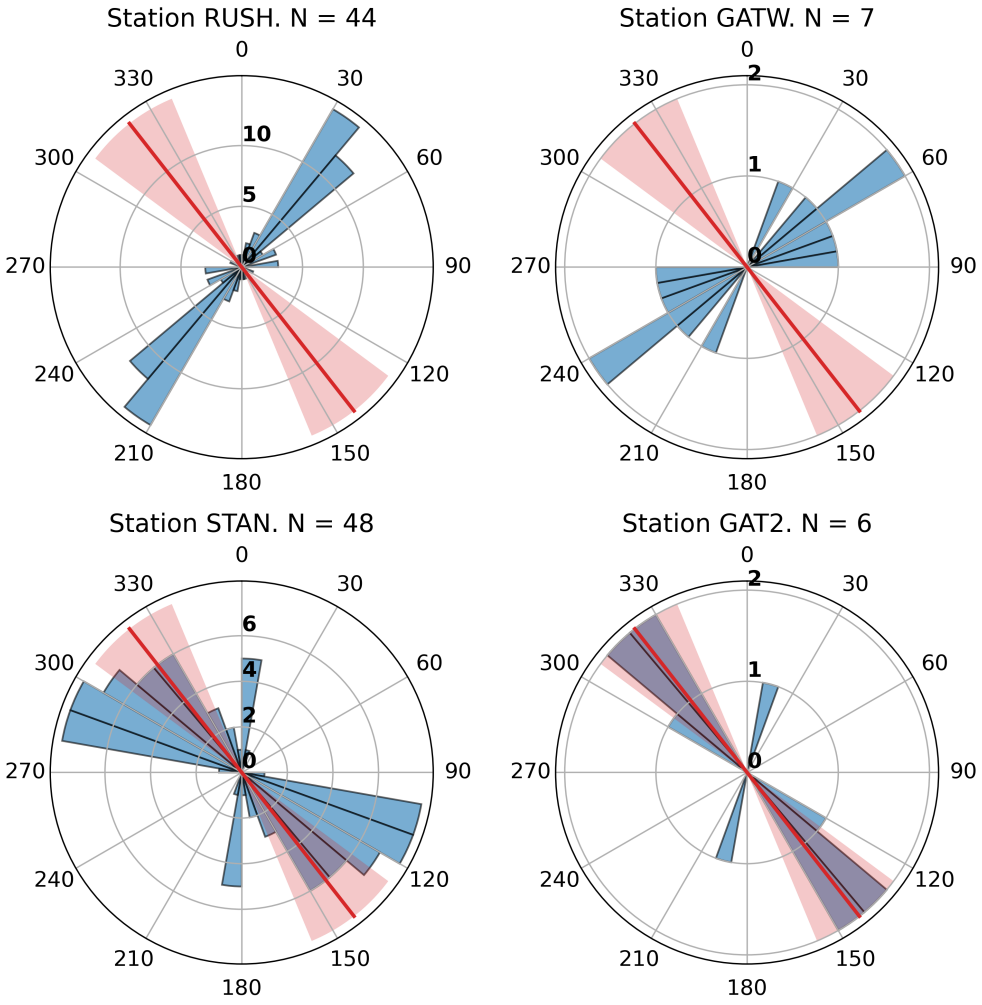

FIGURE 19: Rose histograms of fast polarisation directions measured at 4 stations (RUSH, STAN, GATW and GAT2) at Newdigate, Surrey. Red bar shows the mean regional S_{Hmax} interpreted for the Weald of 142° with a circular standard deviation of 15°.

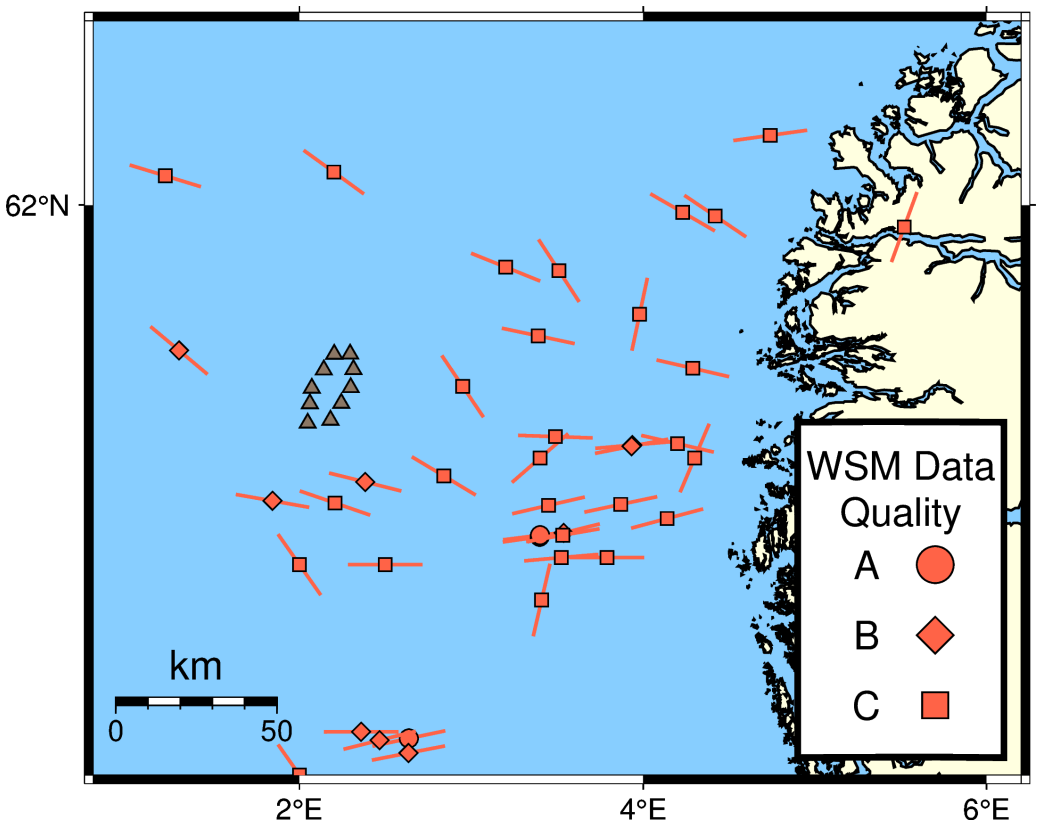

FIGURE 20: Map showing borehole stress data from the World Stress Map database (Heidbach et al., 2016; Heidbach et al., 2018). Bars show the interpreted S_{Hmax} orientation and symbols correspond to data quality where A (circle) has an uncertainty in S_{Hmax} orientation of $< 15°$, B (diamond) has an uncertainty of $< 20°$ and C has an uncertainty $< 25°$. Grey triangles show the location of Snorre PRM stations which share data with the NNSN.

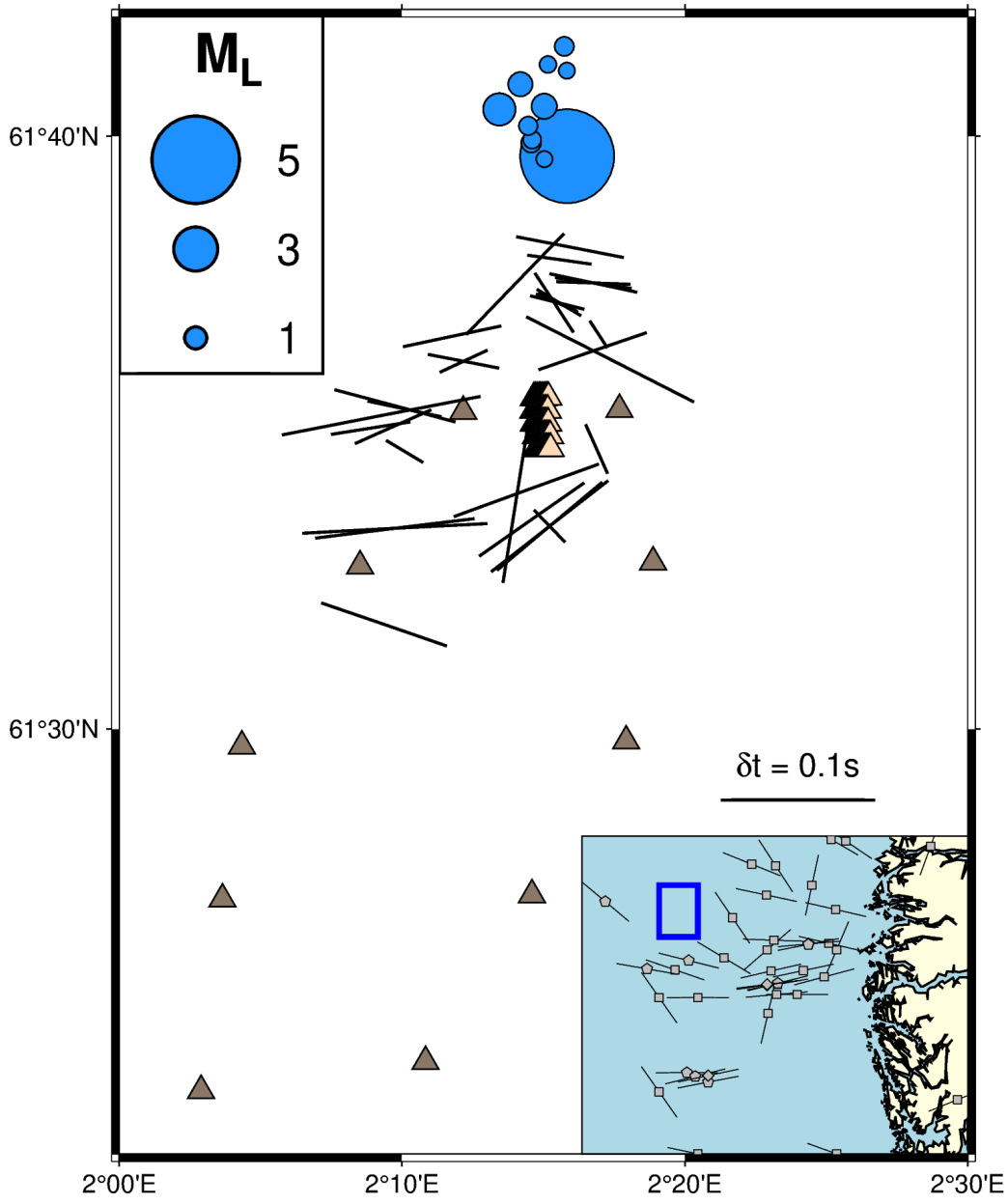

FIGURE 21: Shear-wave splitting measurements for data from permanent reservoir monitoring (PRM) stations (triangles) at the Snorre field. Shear-wave splitting measurements are plotted as in Figure 12. Earthquakes used (blue circles), the 21$_{st}$ March 2022 M_W 5.1 Tampen Spur earthquake and subsequent aftershocks, are plotted at the locations of Jerkins et al. (2024). Data from 10 PRM stations, which is shared with the Norwegian National Seismic Network (Ottemöller et al., 2021), is used for all earthquakes. For the Tampen Spur main-shock, waveform data from an additional 50 PRM stations was provided by Equinor. Inset map shows borehole stress data taken from the World Stress Map data base (Heidbach et al., 2016; Heidbach et al., 2018), plotted as in Figure 20.

5 Implications

Seismic anisotropy, measured using shear-wave splitting, shows promise as a tool to passively measure *in situ* stress in the upper crust. Here we have directly linked shear-wave splitting measurements to borehole measurements of stress using onshore UK data. These case studies highlight the potential for shear-wave splitting to monitor overburden stress, and also a few challenges to both making measurements and interpreting results.

The advantages of shear-wave splitting is that it is a passive measurement and, as such, a few well positioned stations that make a few high quality measurements have the potential to add constraints on the *in situ* stress field at a spatial resolution which cannot be achieved by borehole measurements. At Preston New Road, the closest analogue to monitoring of CO_2 injection where we have data, we measured shear-wave splitting due to stress induced anisotropy. The anisotropy shows no depth dependence, indicating it is only sensitive to the overburden formations, and there it little to no temporal variation in the shear-wave splitting. This suggests that the stress field in the overburden is not changing over the monitoring period. All splitting measurements broadly agree with the regional S_{Hmax}, but by using shear-wave splitting we are able to confirm this is consistently the horizontal stress orientation around the Preston New Road site. This shows the potential for shear-wave splitting measurements made from microseismic monitoring networks to expand spatial sampling of the *in situ* stress field, which adds additional to microseismic monitoring.

A limitation of shear-wave splitting being a passive measurement is that it is dependent on microseismicity occurring within the shear-wave window of monitoring stations. To integrate shear-wave splitting into a monitoring program then the deployment of the microseismic network should include stations where the distance from the station to any potential sources of microseismicity (i.e., a mapped fault or the injector wells) is less than the reservoir depth. Another challenge is that in some localities the seismic anisotropy can be heterogeneous. This is highlighted by the Newdigate case study, where a stark change in measuring shear-wave splitting fast polarisation directions is seen over a short length scale. The Newdigate case study highlights the opportunity that seismic anisotropy offers to monitor temporal variations stress state, if there is sufficient microseismicity to generate shear-wave splitting measurements. At Newdigate, we observed a temporal variation in anisotropy which is best explained by a stress build up and release during the Newdigate earthquake swarm. Further analysis, such as measuring frequency-dependent anisotropy and inverting shear-wave splitting measurements to test for multiple fracture networks is planned. In the CO_2 monitoring context, where other supplementary datasets such as 3-D seismic and borehole logs are available, we would expect this issue of interpretation uncertainty to be greatly reduced.

The primary challenge for our onshore study is amassing sufficient data in a region, as data attrition is an issue in shear-wave splitting studies at all scales. Whilst the UK is well instrumented, deployments are not designed with the restrictions of the shear-wave window in mind. We see the corollary to this for our offshore datasets, where sensors are deployed to monitor particular fields. We are only able to make a meaningful number of shear-wave splitting measurements for Permanent Reservoir Monitoring (PRM) stations at Snorre, as the other fields and the OBS deployment in the Skagerrak have few or no earthquakes within the shear-wave window. At Snorre, our result show that PRM systems

are highly suitable for measuring shear-wave splitting for microseismic events. We also see the advantage of a dense monitoring network, where even the few earthquakes used at Snorre generates a dataset which suggest we primarily see stress-induced anisotropy with a stress orientation that is consistent with the regional stress field.

The offshore results show that shear-wave splitting measurements are feasible for CO_2 storage monitoring, with our onshore results showing that shear-wave splitting for near-surface (ca. 1 − 2 km depth) microseismic events is capable of resolving stress-induced seismic anisotropy. However, some of the complexities highlighted by our onshore study mean that shear-wave splitting is most suitable for increasing sample density for regions where nearby borehole stress data is available or for monitoring changes in anisotropy over time which may be indicative of changes in stress in the overburden. Furthermore there is potential to improve the links between shear-wave splitting measurements and geomechanical reservoir models, which would further increase the value of incorporating shear-wave splitting analysis into monitoring frameworks.

5.1 Monitoring

As this report highlights, anisotropy measurements from shear-wave splitting analysis are made possible by having seismic stations above the earthquake sources. This means that offshore passive seismic monitoring would be required to conduct this type of analysis in the immediate vicinity of CO_2 storage sites.

Employing offshore monitoring methods purely for anisotropy analysis alone would be unlikely due to economic constraints. However, offshore passive seismic monitoring in some form is likely to be included in project plans for detecting and locating natural and induced seismicity near storage sites. Shear-wave splitting analysis could be readily employed on appropriate data collected from these offshore systems, giving added value and an additional, independent means of detecting geomechanical changes in and around storage reservoirs. The potential to use seismic anisotropy to monitor temporal variations in stress state in the reservoir and overburden could constitute an important source additional value to any offshore monitoring program if the offshore monitoring is designed with the constraints of shear-wave splitting (i.e., the shear-wave window limitation) in mind.

The passive seismic data will need to be of an appropriate type (e.g., three-component), meaning single-component fibre-optic distributed acoustic sensing (DAS) data may not be usable for full seismic anisotropy analysis, depending on the geometry of its deployment. However, shear-wave splitting does not require accurately calibrated instrument response functions and coupling constants, which can often pose difficulties for other seismological analyses using offshore data. Ocean bottom seismometers or permanent reservoir monitoring type systems would be the most suitable instrumentation, as demonstrated in this report, along with borehole geophones.

6 Summary

In this report we review seismic anisotropy and the potential for measuring stress-induced seismic anisotropy using shear-wave splitting. Additional means of constraining stress or fracturing across the CO_2 storage complex are valuable, particularly those that are independent means of imaging the reservoir, seal, and overburden units. Using onshore passive seismic and stress data for the UK, we show that shear-wave splitting is primarily sensitive to stress-induced alignment of cracks which allows us to constrain the orientation of S_{Hmax}. In South East England, we observe a change in anisotropy across the Newdigate fault and a temporal variation in anisotropy during the Newdigate earthquake sequence. This highlights the potential for shear-wave splitting to measure temporal variations in the stress field.

As shear-wave splitting is a passive measurement, it gives the potential to make semi-continuous measurements of the stress field in the caprock and overburden units, provided there is sufficient microseismcity in underlying formations or the basement. Offshore measurements, using data from Permanent Reservoir Monitoring (PRM) systems at the Snorre field, show that PRM systems are highly suitable for measuring shear-wave splitting if there are offshore seismic stations deployed above CO_2 storage projects. This makes shear-wave splitting an important potential added value that should be considered when planning offshore passive seismic monitoring of CO_2 storage projects.

References

Asplet, Joseph, James Wookey, and Michael Kendall (2023). "Inversion of shear wave waveforms reveal deformation in the lowermost mantle". In: *Geophysical Journal International* 232.1, pp. 97–114.

Asplet, Joseph, James Wookey, Micheal Kendall, Mark Chapman, and Ritima Das (May 2024). "Shear-wave attenuation anisotropy: a new constraint on mantle melt near the Main Ethiopian Rift". In: *Seismica* 3.1. Section: Articles. DOI: 10.26443/seismica.v3i1.1098.

Backus, George E. (1962). "Long-wave elastic anisotropy produced by horizontal layering". In: *Journal of Geophysical Research* 67.11, pp. 4427–4440. ISSN: 0148-0227. DOI: 10.1029/jz067i011p04427.

Baird, Alan F., J.-Michael Kendall, R. Stephen J. Sparks, and Brian Baptie (2015). "Transtensional deformation of Montserrat revealed by shear wave splitting". In: *Earth and Planetary Science Letters* 425, pp. 179–186. ISSN: 0012-821X. DOI: 10.1016/j.epsl.2015.06.006.

Baird, Alan F., J.-Michael Kendall, James P. Verdon, Andreas Wuestefeld, Todd E. Noble, Yongyi Li, Martin Dutko, and Quentin J. Fisher (2013). "Monitoring increases in fracture connectivity during hydraulic stimulations from temporal variations in shear wave splitting polarization". In: *Geophysical Journal International* 195.2, pp. 1120–1131. ISSN: 0956-540X. DOI: 10.1093/gji/ggt274.

Bell, J. S. and D. I. Gough (Nov. 1979). "Northeast-southwest compressive stress in Alberta evidence from oil wells". In: *Earth and Planetary Science Letters* 45.2, pp. 475–482. ISSN: 0012-821X. DOI: 10.1016/0012-821X(79)90146-8.

Boness, Naomi L. and Mark D. Zoback (Oct. 2006). "Mapping stress and structurally controlled crustal shear velocity anisotropy in California". In: *Geology* 34.10, pp. 825–828. ISSN: 0091-7613. DOI: 10.1130/G22309.1.

Booth, David C and Stuart Crampin (1985). "Shear-wave polarizations on a curved wavefront at an isotropic free surface". In: *Geophysical Journal International* 83.1, pp. 31–45.

British Geological Survey (1970). *Great Britain Seismograph Network*. DOI: 10.7914/AV8J-NC83.

British Geological Survey (2015). *UKArray*. DOI: 10.7914/SN/UR.

Castellazzi, Claire, Martha K Savage, Ernestynne Walsh, and Richard Arnold (2015). "Shear wave automatic picking and splitting measurements at Ruapehu volcano, New Zealand". In: *Journal of Geophysical Research: Solid Earth* 120.5, pp. 3363–3384.

Chapman, M (2003). "Frequency-dependent anisotropy due to meso-scale fractures in the presence of equant porosity". In: *Geophysical Prospecting* 51.5, pp. 369–379. ISSN: 1365-2478. DOI: 10.1046/j.1365-2478.2003.00384.x.

Clarke, Huw, Hamed Soroush, and Thomas Wood (2019a). "Preston New Road: The Role of Geomechanics in Successful Drilling of the UK's First Horizontal Shale Gas Well". In: *SPE Europec featured at 81st EAGE Conference and Exhibition*, D041S012R008. DOI: 10.2118/195563-ms.

Clarke, Huw, James P Verdon, Tom Kettlety, Alan F Baird, and J-Michael Kendall (2019b). "Real-time imaging, forecasting, and management of human-induced seismicity at Preston New Road, Lancashire, England". In: *Seismological Research Letters* 90.5, pp. 1902–1915.

Crampin, S (1999). "Calculable fluid–rock interactions". In: *Journal of the Geological Society* 156.3, pp. 501–514. ISSN: 0016-7649. DOI: 10.1144/gsjgs.156.3.0501.

Crampin, Stuart (1978). "Seismic-wave propagation through a cracked solid: polarization as a possible dilatancy diagnostic". In: *Geophysical Journal International* 53.3, pp. 467–496.

Crampin, Stuart and Sheila Peacock (Jan. 2005). “A review of shear-wave splitting in the compliant crack-critical anisotropic Earth”. In: *Wave Motion* 41.1, pp. 59–77. ISSN: 0165-2125. DOI: 10.1016/j.wavemoti.2004.05.006.

Crampin, Stuart, Theodora Volti, and Ragnar Stefánsson (1999). “A successfully stress-forecast earthquake”. In: *Geophysical Journal International* 138.1, F1–F5. ISSN: 0956-540X. DOI: 10.1046/j.1365-246x.1999.00891.x.

Al-Harrasi, O. H., J.-M. Kendall, and M. Chapman (2011). “Fracture characterization using frequency-dependent shear wave anisotropy analysis of microseismic data”. In: *Geophysical Journal International* 185.2, pp. 1059–1070. ISSN: 1365-246X. DOI: 10.1111/j.1365-246x.2011.04997.x.

Heidbach, O, Andreas Barth, Birgit Müller, John Reinecker, Ove Stephansson, Mark Tingay, and A Zang (2016). “WSM quality ranking scheme, database description and analysis guidelines for stress indicator”. In: *World Stress Map Technical Report 16-01*.

Heidbach, Oliver et al. (Oct. 2018). “The World Stress Map database release 2016: Crustal stress pattern across scales”. In: *Tectonophysics* 744, pp. 484–498. ISSN: 0040-1951. DOI: 10.1016/j.tecto.2018.07.007.

Hicks, Stephen P., James Verdon, Brian Baptie, Richard Luckett, Zoë K. Mildon, and Thomas Gernon (2019). “A Shallow Earthquake Swarm Close to Hydrocarbon Activities: Discriminating between Natural and Induced Causes for the 2018–2019 Surrey, United Kingdom, Earthquake Sequence”. In: *Seismological Research Letters* 90.6, pp. 2095–2110. ISSN: 0895-0695. DOI: 10.1785/0220190125.

Hudson, J. A. (1981). “Wave speeds and attenuation of elastic waves in material containing cracks”. In: *Geophysical Journal of the Royal Astronomical Society* 64.1, pp. 133–150. ISSN: 1365-246X. DOI: 10.1111/j.1365-246x.1981.tb02662.x.

Hudson, Thomas Samuel, Tom Kettlety, John-Michael Kendall, Tom O’Toole, Andrew Jupe, Robin K Shail, and Augusta Grand (2024). “Seismic Node Arrays for Enhanced Understanding and Monitoring of Geothermal Systems”. In: *The Seismic Record* 4.3, pp. 161–171.

Hurd, Owen and Marco Bohnhoff (2012). “Stress-and structure-induced shear-wave anisotropy along the 1999 Izmit rupture, Northwest Turkey”. In: *Bulletin of the Seismological Society of America* 102.5, pp. 2177–2188.

Igonin, Nadine, James P Verdon, and David W Eaton (2022). “Seismic Anisotropy Reveals Stress Changes around a Fault as It Is Activated by Hydraulic Fracturing”. In: *Seismological Research Letters* 93.3, pp. 1737–1752. ISSN: 0895-0695. DOI: 10.1785/0220210282.

Illsley-Kemp, Finnigan, Martha K Savage, Colin JN Wilson, and Stephen Bannister (2019). “Mapping stress and structure from subducting slab to magmatic rift: Crustal seismic anisotropy of the North Island, New Zealand”. In: *Geochemistry, Geophysics, Geosystems* 20.11, pp. 5038–5056.

Jerkins, Annie E., Volker Oye, Celso Alvizuri, Felix Halpaap, and Tormod Kværna (Apr. 2024). “The 21 March 2022 Mw 5.1 Tampen Spur Earthquake, North Sea: Location, Moment Tensor, and Context”. en. In: *Bulletin of the Seismological Society of America* 114.2, pp. 741–757. ISSN: 0037-1106, 1943-3573. DOI: 10.1785/0120230163.

Jin, Zhaoyu, Mark Chapman, and Giorgos Papageorgiou (2018). “Frequency-dependent anisotropy in a partially saturated fractured rock”. In: *Geophysical Journal International* 215.3, pp. 1985–1998. ISSN: 0956-540X. DOI: 10.1093/gji/ggy399.

Kendall, J-M, QJ Fisher, S Covey Crump, J Maddock, A Carter, SA Hall, J Wookey, SLA Valcke, M Casey, G Lloyd, et al. (2007). "Seismic anisotropy as an indicator of reservoir quality in siliciclastic rocks". In: *Geological Society, London, Special Publications* 292.1, pp. 123–136.

Kendall, J-M, T Terakawa, M Savage, T Kettley, D Minifie, H Nakamichi, and A Wuestefeld (2024, in revision). "Changes in seismic anisotropy at Ontake volcano: a tale of two eruptions". In: *Seismica*.

Kettley, Tom, James P Verdon, Antony Butcher, Matthew Hampson, and Lucy Craddock (2020). "High-Resolution Imaging of the ML 2.9 August 2019 Earthquake in Lancashire, United Kingdom, Induced by Hydraulic Fracturing during Preston New Road PNR-2 Operations". In: *Seismological Research Letters* 92.1, pp. 151–169. ISSN: 0895-0695. DOI: 10.1785/0220200187.

Kettley, Tom et al. (May 2024). "A Unified Earthquake Catalogue for the North Sea to Derisk European CCS Operations". en. In: *First Break* 42.5, pp. 31–36. ISSN: 0263-5046, 1365-2397. DOI: 10.3997/1365-2397.fb2024036.

Kingdon, Andrew, Mark W. Fellgett, and John D. O. Williams (2016). "Use of borehole imaging to improve understanding of the in-situ stress orientation of Central and Northern England and its implications for unconventional hydrocarbon resources". In: *Marine and Petroleum Geology* 73, pp. 1–20. ISSN: 0264-8172. DOI: https://doi.org/10.1016/j.marpetgeo.2016.02.012.

Kingdon, Andrew, John Williams, Mark Fellgett, Naomi Rettelbach, and Oliver Heidbach (2022). "Stress Map of Great Britain and Ireland 2022". In.

Klein, RJ and MV Barr (Sept. 1986). "Regional state of stress in western Europe". In: *Proceedings of the International Symposium on Rock Stress and Rock Stress Measurements, Stockholm*. Ed. by O Stephansson. ISRM. Centek, Lulea, pp. 33–44.

Link, Frederik and Maureen D Long (2024). "SItomo–A toolbox for splitting intensity tomography and application in the Eastern Alps". In: *Journal of Geodynamics* 159, p. 102018.

Liu, Sha, Stuart Crampin, Richard Luckett, and Jiansi Yang (Oct. 2014). "Changes in shear wave splitting before the 2010 Eyjafjallajökull eruption in Iceland". In: *Geophysical Journal International* 199.1, pp. 102–112. ISSN: 0956-540X. DOI: 10.1093/gji/ggu202.

Nuttli, Otto (1961). "The effect of the Earth's surface on the S wave particle motion". In: *Bulletin of the Seismological Society of America* 51.2, pp. 237–246.

Ottemöller, Lars, Jan Michalek, Jon-Magnus Christensen, Ulf Baadshaug, Felix Halpaap, Øyvind Natvik, Tormod Kværna, and Volker Oye (Jan. 2021). "UiB-NORSAR EIDA Node: Integration of Seismological Data in Norway". In: *Seismological Research Letters* 92.3, pp. 1491–1500. ISSN: 0895-0695. DOI: 10.1785/0220200369.

Plumb, Richard A. and Stephen H. Hickman (1985). "Stress-induced borehole elongation: A comparison between the four-arm dipmeter and the borehole televiewer in the Auburn Geothermal Well". In: *Journal of Geophysical Research: Solid Earth* 90.B7, pp. 5513–5521. DOI: https://doi.org/10.1029/JB090iB07p05513.

Savage, M. K., A. Wessel, N. A. Teanby, and A. W. Hurst (2010a). "Automatic measurement of shear wave splitting and applications to time varying anisotropy at Mount Ruapehu volcano, New Zealand". In: *Journal of Geophysical Research: Solid Earth* 115.B12. DOI: https://doi.org/10.1029/2010JB007722.

Savage, Martha K, Takao Ohminato, Yosuke Aoki, Hiroshi Tsuji, and Sonja M Greve (2010b). "Stress magnitude and its temporal variation at Mt. Asama Volcano, Japan, from seismic anisotropy and GPS". In: *Earth and Planetary Science Letters* 290.3-4, pp. 403–414.

Silver, Paul G and W Winston Chan (1991). "Shear wave splitting and subcontinental mantle deformation". In: *Journal of Geophysical Research: Solid Earth* 96.B10, pp. 16429–16454.

Stork, Anna L., James P. Verdon, and J.-Michael Kendall (Jan. 2015). "The microseismic response at the In Salah Carbon Capture and Storage (CCS) site". In: *International Journal of Greenhouse Gas Control* 32, pp. 159–171. ISSN: 1750-5836. DOI: 10.1016/j.ijggc.2014.11.014.

Teanby, N., J.-M. Kendall, R. H. Jones, and O. Barkved (Mar. 2004a). "Stress-induced temporal variations in seismic anisotropy observed in microseismic data". In: *Geophysical Journal International* 156.3. _eprint: https://academic.oup.com/gji/article-pdf/156/3/459/5883127/156-3-459.pdf, pp. 459–466. ISSN: 0956-540X. DOI: 10.1111/j.1365-246X.2004.02212.x.

Teanby, Nicholas A, J-M Kendall, and M Van der Baan (2004b). "Automation of shear-wave splitting measurements using cluster analysis". In: *Bulletin of the Seismological Society of America* 94.2, pp. 453–463.

Thompson, M, M Andersen, RM Elde, SS Roy, and SM Skogland (2015). "Delivering permanent reservoir monitoring for Snorre and Grane". In: *Third EAGE Workshop on Permanent Reservoir Monitoring 2015*. Vol. 2015. 1. European Association of Geoscientists & Engineers, pp. 1–5.

Verdon, J. P., J.-M. Kendall, and Andreas Wüstefeld (2009). "Imaging fractures and sedimentary fabrics using shear wave splitting measurements made on passive seismic data". In: *Geophysical Journal International* 179.2. Publisher: Blackwell Publishing Ltd Oxford, UK, pp. 1245–1254.

Verdon, James P and J-Michael Kendall (2011). "Detection of multiple fracture sets using observations of shear-wave splitting in microseismic data". In: *Geophysical Prospecting* 59.4, pp. 593–608.

Volti, T and S Crampin (2003). "A four-year study of shear-wave splitting in Iceland: 2. Temporal changes before earthquakes and volcanic eruptions". In: *Geological Society, London, Special Publications* 212.1, pp. 135–149.

Walsh, E., R. Arnold, and M. K. Savage (Oct. 2013). "Silver and Chan revisited". In: *Journal of Geophysical Research: Solid Earth* 118.10, pp. 5500–5515. ISSN: 21699313. DOI: 10.1002/jgrb.50386.

Wookey, James (2012). "Direct probabilistic inversion of shear wave data for seismic anisotropy". In: *Geophysical Journal International* 189.2, pp. 1025–1037. ISSN: 0956540X. DOI: 10.1111/j.1365-246x.2012.05405.x.

Wuestefeld, Andreas, Othman Al-Harrasi, James P Verdon, James Wookey, and J Michael Kendall (2010). "A strategy for automated analysis of passive microseismic data to image seismic anisotropy and fracture characteristics". In: *Geophysical Prospecting* 58.5, pp. 755–773.